

# BehaVR: User Identification Based on VR Sensor Data

Ismat Jarin\* Yu Duan\* Rahmadi Trimananda Hao Cui Salma Elmalaki Athina Markopoulou  
University of California, Irvine

**Abstract**—Virtual reality (VR) platforms enable a wide range of applications, however pose unique privacy risks. In particular, VR devices are equipped with a rich set of sensors that collect personal and sensitive information (e.g., body motion, eye gaze, hand joints, and facial expression), which can be used to uniquely identify a user, even without explicit identifiers. In this paper, we are interested in understanding the extent to which a user can be identified based on data collected by different VR sensors. We consider adversaries with capabilities that range from observing APIs available within a single VR app (app adversary) to observing all, or selected, sensor measurements across all apps on the VR device (device adversary).

To that end, we introduce BEHAVR, a framework for collecting and analyzing data from *all* sensor groups collected by *all* apps running on a VR device. We use BEHAVR to perform a user study and collect data from real users that interact with popular real-world apps. We use that data to build machine learning models for user identification, with features extracted from sensor data available within and across apps. We show that these models can identify users with an accuracy of up to 100%, and we reveal the most important features and sensor groups, depending on the functionality of the app and the strength of the adversary, as well as the minimum time needed for user identification. To the best of our knowledge, BEHAVR is the first to analyze user identification in VR comprehensively, *i.e.*, considering jointly all sensor measurements available on a VR device (whether within an app or across multiple apps), collected by real-world, as opposed to custom-made, apps.

## 1. Introduction

Virtual reality (VR) is a large and growing market [44] that enables a wide range of applications, from gaming to education [36] and work [33]. As of April 2023, the Meta Quest Store has 441 VR apps [4] and by the end of July 2023, the Steam app store has over 5,600 VR apps [51]—these are two major app stores for VR apps. The VR ecosystem also comes with privacy concerns. Recent work showed that Oculus VR and its apps already collect personally identifying information [57], and can further infer sensitive attributes [42]. Some of this tracking and profiling are similar to practices in other app ecosystems, such as mobile [13], [48], smart TV [41], [61], web [9],

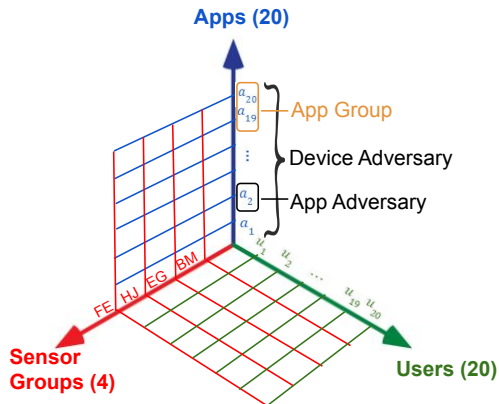


Figure 1: The problem space of user identification spans several dimensions: users, apps, and sensors. We consider four sensor groups: body motion (BM), eye gaze (EG), hand joints (HJ), facial expression (FE). We consider two types of adversaries: the app adversary has access only to one app; the device adversary has access across multiple apps. We further define groups of apps with similar activities and emotional states.

etc. with some differences: the VR ecosystem is younger, more centralized, and not driven by ads, yet [57].

**User Identification.** In addition, VR poses a novel and powerful threat to privacy, by leveraging a rich set of sensors that capture sensitive, deeply personal information. Modern VR devices (e.g., Meta Quest Pro), including their headsets and controllers, are equipped with sensors that collect measurements about head and body motion (“BM”) [25], [37], eye gaze (“EG”) [21], [34], hand joints (“HJ”) [22], [35], and facial expression (“FE”) [24], [38]. All these measurements are available on the device itself (e.g., Quest Pro), can be sent to the platform (Meta), and a subset can be made available to VR app developers via APIs as needed. Recent works [39], [43] have shown that some of these measurements can indeed be used for unique identification. The privacy implication is that a user’s behavior in VR creates fingerprints<sup>1</sup> that can be used to identify users in the virtual world (even if they use different accounts or avatars in the same app, and across different apps or devices), and potentially in the real world as well (e.g., if motion/eye/face

1. The combination of features extracted from the VR sensor data streams can produce unique (quasi-)identifiers/fingerprints, including biometrics [7] and behavioral biometrics (or “behaviometrics”) [46], [53].

\*. The two authors made equal contributions and share first authorship.

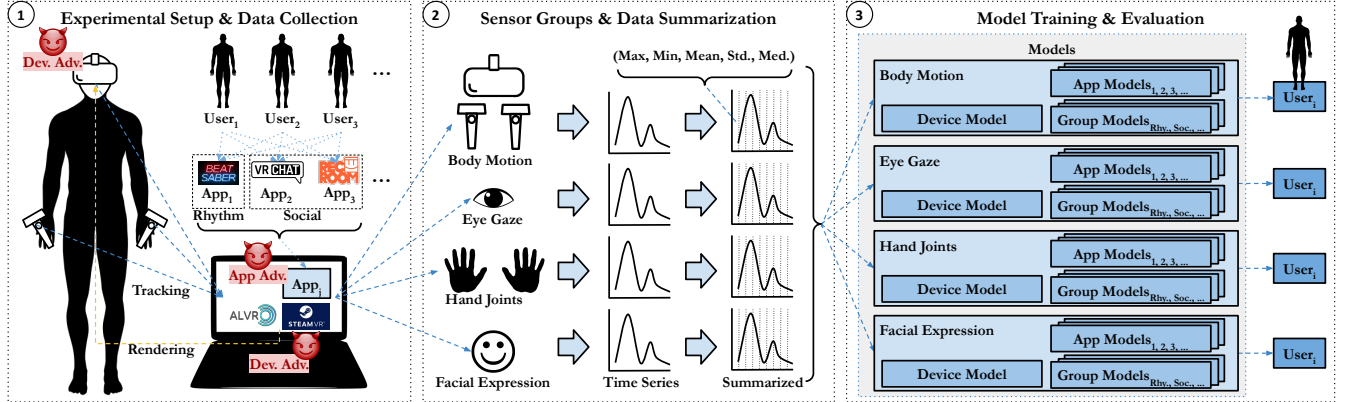


Figure 2: **Overview of BEHAVR.** (1) **Data Collection Setup:** every user interacts with each app using Quest Pro; each app (e.g., Beat Saber) runs on a PC and its VR environment is rendered on the Quest Pro headset; this enables the recording of sensor data sent from Quest Pro to the PC; apps are grouped based on similarity of activities and emotional states. (2) **Data Processing:** there are four groups of sensors, namely *body motion*, *hand joints*, *eye gaze*, and *facial expression*; we divide the time series generated by every sensor group into blocks, and we compute 5 *statistics* per block as features. (3) **Model Training & Evaluation:** using the previous features per block, we train different models (using data per app, across apps, even per group of apps) that an adversary can use to uniquely identify users.

data are captured and matched by a surveillance camera).

In this paper, we broadly refer to the sensor measurements collected on VR devices, as well as to features extracted from them, as VR sensor data. We are interested in understanding *to what extent a user can be uniquely identified based on VR sensor data*; and which are the top features, across all sensor groups and real-world apps, for a passive adversary that wants to uniquely identify a user with minimal effort. In particular, we consider two types of adversaries, depending on their vantage point for access to sensor data: (1) the *app adversary* mimics an app developer who has access to sensor data from APIs available within the app; and (2) the *device adversary* can have access to all sensor data collected on the device and mimics the VR device (see Section 2.4 for the adversarial models). The full problem space we consider is depicted in Fig. 1.

Prior work has studied only parts of this problem space. In particular, user identification has been demonstrated based on body motion (e.g., positional and rotational) sensor data from VR headsets and controllers [39], [43], [56]; this corresponds to the BM sensor group in our problem space. Newer headsets, such as the Meta Quest Pro and the Apple Vision Pro, also offer more comprehensive tracking of body parts like eyes, hands, and face [34], [38], [63]. Privacy aspects of these APIs are receiving increasing attention [29], [42], but their use for identification has not been studied yet. Furthermore, all prior identification studies were limited to measurements collected using APIs within a single app, either a real-world app (e.g., Beat Saber in [43]) or a custom app with tasks specifically designed for user studies [39], [42], [56]; these studies consider our app adversary model.

**Approach.** We introduce BEHAVR, a framework for collecting and analyzing data from all available sensor groups (i.e., body motion, eye gaze, hand joints, and facial expres-

sion), and performing user identification within (i.e., app adversary) and across (i.e., device adversary) apps. To the best of our knowledge, BEHAVR is the first to analyze user identification in VR comprehensively, i.e., considering *all* sensor measurements available on a VR device, and *all* apps running on the device. Fig. 2 presents the overview of BEHAVR. Next, we describe the BEHAVR components and we highlight methodological contributions along the way.

(1) *Collection of sensor data from all apps on the VR device.* We develop an approach that enables us to observe, for the first time, all sensor data collected by all real-world apps. To that end, we leverage the SteamVR setup (i.e., each app runs on a PC and its VR environment is rendered on the Quest Pro headset), which was originally introduced to boost performance. We use ALVR [2] in a novel way to record all sensor data by listening to the API calls. This gives visibility into data collected by all (not just one) apps, including real-world (not just custom) apps running unmodified on the device, which was not previously possible.

Using the BEHAVR setup, we perform a user study and collect a comprehensive dataset which includes all four sensor groups, from 20 users interacting with 20 most popular real-world apps on the SteamVR store (see Section 3).

(2) *Data Analysis.* One challenge worth highlighting is how to process VR sensor data into time blocks for model training. Most prior work asked users to perform specific tasks, and trained models on fixed time blocks and/or anchored around the defined tasks in [39], [43]. We introduce a new time-based approach that fixes the block amount, taking into account the variability in the time it takes for different users to play different apps. Our rough time scaling is intuitive but robust and provides good identification performance on real-world apps (see Section 4).

(3) *Feature Engineering and Model Training.* For each time

block, we summarize statistics within that block, following the approach in [39] [43]. Then, we train a user classification model (*e.g.*, Random Forest) per sensor group; finally we combine labels of each block using the maximum-voting approach in [39]. To the best of our knowledge, this paper is the first to explore not only body motion and eye gaze data, but also each of the hand joints and facial expression sensor groups for user identification in VR, as well as to compare and combine across sensor groups and apps. In addition to the standard features extracted from the VR sensor streams [39] [43], we also perform augmentation: for eye gaze, we introduce new features that correlate left and right eye’s data; selection: for facial expression, we explore facial elements and their combinations that represent users’ emotions [15], [24] when interacting with an app. Finally, we define groups based on similarity of activities and induced emotional states; we train a model per app group per sensor group, which allows us to identify users across apps in the same app group (see section 2.1).

**Identification Results.** We apply BEHAVR to investigate how well users can be identified from their VR sensor data. Section 5 presents a comprehensive evaluation across sensor groups, apps or groups of apps, and adversary models, guided by the following research questions (RQ).

*RQ1: How well can a user be identified using VR sensor data from a particular sensor group?* We find that the app adversary can achieve up to 100% accuracy for many apps, especially using data from facial expression and body motion sensor groups that perform better than eye gaze and hand joints. For most sensor groups, the device adversary achieves 100% accuracy, using data from multiple/all apps.

*RQ2: How long does it take to identify a user?* We find that the app adversary generally requires around 18–20 seconds of data across body motion and facial expression sensor groups for up to 90% accuracy, and ~50 seconds for eye gaze for up to 85% accuracy. The device adversary requires less data (~9s average), since it combines data across apps.

*RQ3: What are the top features for identification?* We find that, for the app adversary, the top features describe the unique interaction between the user and the VR environment. For the device adversary, the top features describe unique physical characteristics (*e.g.*, height, inter-pupillary distance (IPD)) that can identify users across apps.

*RQ4: Can we identify a user across different apps?* We consider training models based on the sensor data from one or more apps, and we attempt to identify the same user on a different (“zero-day”) app. In Section 2.1, we define groups of apps, based on similar activities (*e.g.*, social, flight simulation, shooting, and rhythm apps) and emotional states. We find that, depending on the sensor group, the models can give up to 100% accuracy when identifying users for another app within the same app group, but much worse when identifying users in apps of a different group.

*RQ5: What are the most important sensor groups for identification?* We find that different sensor groups are important to different types of apps based on activity and emotions. For example, shooting and rhythm apps require users to move

their heads and controllers a lot; thus, body motion plays an important role in identification in these apps.

**Overview.** The rest of the paper is structured as follows. Section 2 provides background and the problem setup. Section 3 presents the experimental setup and data collection. Section 4 presents the data analysis and model training. Section 5 presents the evaluation results for app and device adversaries, for all sensor group and groups of apps. Section 6 reviews related work. Section 7 provides discussion and conclusion. The appendices provides additional results.

## 2. Background and Problem Setup

### 2.1. VR Apps

**App Store.** We look into VR apps available on the Steam app store, one of the most popular online app stores [59]. It provides apps (typically games) for various platforms, including PC and VR, with support for various VR devices, such as those from Oculus and HTC. At peak times, accumulates more than 30 million users [50]. SteamVR is a plugin that allows users to run Steam apps that provide VR support on their VR devices [60]. BEHAVR leverages SteamVR to run apps and ALVR [2] to record all sensor data by listening to the API calls (see Section 3).

**App Selection.** Starting from the top 100 apps from the “Most played VR games” list on Steam [52], we select 20 representative VR apps based on several criteria. First, we exclude apps that may cause inconvenience to most users, *e.g.*, games of the horror genre, games that exhibit too much violence, etc. This first criterion is mandated in 45 CFR § 46.111(a)(1) to minimize the experimental risk (*e.g.*, physical or psychological harm) on our study participants [19]. Second, we also exclude apps that do not have full VR support, *e.g.*, a number of apps work only on VR devices other than Quest Pro, or they require a combination of VR controllers and PC keyboard as input devices. Finally, we attempt to compile a rich set of apps from various genres, *e.g.*, rhythm, flying simulation, shooting, etc. The list of 20 SteamVR apps is shown in Table 4 in Appendix A, and they are referred to as  $a_1, \dots, a_{20}$ , throughout the paper.

**Apps Grouping.** We further group apps based on their similarity of activities and emotional states. Our motivation is to leverage the similarity of apps for user identification, *i.e.*, use data and training on data from multiple similar apps, to better identify users on apps within the same group. In addition, if there are data from any new app, the adversary only needs to retrain the group model instead of retraining with all app’s data which is intuitively more resource-efficient. Although heuristic, our app grouping performs well (see Section 5.5.1 and Table 2) in user identification and serves as proof of concept; an adversary can further optimize it.

We propose our grouping in Table 1. For body motion and hand joints, we group apps according to similar app-specific activities. For example, social apps typically make users to walk, wave, and look around; in contrast, shooting apps require users to target and shoot objects, which lead to

TABLE 1: Grouping apps ( $a_1, \dots, a_{20}$  listed in in Table 4 in Appendix A) based on their similarity of activities and emotional states (arousal/valence). *Sensor Groups*: BM, EG, HJ, FE. *Emotional States*: LA = low arousal, HA = high arousal, PV = positive valence, NV = negative valence.

App Groups	App No.	App-Specific Activities	Arousal/Valence	Important Sensors
Social	$a_{12}, a_{15}, a_{18}$	Walking, waving, grabbing and sightseeing	LA/PV, HA/PV	BM, EG, FE
Flight Simulation	$a_3, a_{19}, a_{20}$	Holding onto the airplane control stick, interacting with control panel/buttons in an airplane cockpit	LA/NV, HA/NV, LA/PV	BM, EG, HJ, FE
Golfing	$a_6$	Walking, holding a golf stick, and hit the ball slowly	LA/PV, HA/PV	BM
Interactive Navigation	$a_2, a_9, a_{10}, a_{11}, a_{16}, a_{17}$	Grabbing, moving objects, opening doors, <i>i.e.</i> , short time interaction with objects	Neutral, LA/PV, LA/NV	BM, EG, HJ
Knuckle-walking	$a_7$	Walking using an open fist like a gorilla	LA/PV, HA/PV, LA/NV	BM, HJ, FE
Rhythm	$a_1$	Dancing-like moves and cutting objects in quick pace	All	BM, EG, HJ, FE
Shooting & Archery	$a_{13}, a_{14}, a_5$	Grabbing and holding a gun/arrow, aiming and shooting at objects	LA/NV, HA/NV	BM, EG, FE, HJ
Teleportation	$a_4, a_8$	Teleporting, mostly standing up, <i>i.e.</i> , without moving much	All	FE

different motion patterns. However, even within the same group, differences exist; *e.g.*, in the shooting group,  $a_{13}$  requires teleporting, while  $a_{14}$  requires walking.

For facial expression only, the grouping further considers emotional *arousal* (*e.g.*, how calm or active an emotion is) and *valence* (*i.e.*, how positive or negative an emotion is) states afforded by the VR environment of an app; we use the approach proposed in [6], [28], [54]. There are four types of arousal-valence states we can consider, namely high arousal positive valence (HA/PV), *e.g.*, happiness; low arousal positive valence (LA/PV), *e.g.*, surprise; high arousal negative valence (HA/NV), *e.g.*, fear/stress; and finally low arousal negative valence (LA/NV), *e.g.*, sadness. For example, we observe that social apps induce mostly joy or surprise (*i.e.*, HA/PV), and flying simulation or shooting apps induce mostly fear/stress (*i.e.*, HA/NV). Furthermore, one app can induce multiple emotions depending on the situation (*e.g.*, when completing a level in a game, users feel happy if they succeed and sad if they fail).

The last column in Table 1 lists the important sensor groups for each app group. Throughout our data collection, all sensors remain active, but specific apps may have certain sensor groups with more activities; *i.e.*, in a teleportation app, users utilize the controllers to teleport in VR environment, resulting in less activities detected by body motion sensors. In a flight simulation app, users move their body, use their hands to interact with the objects, and look at control panel. Thus, body motion, eye gaze, and hand joints are listed as the important sensor groups for this app group. The importance of these sensor groups for user identification is confirmed in the evaluation (see Section 5.5.3).

## 2.2. Sensor Groups

We explore all VR sensor data available today, *i.e.*, the following four groups: body motion [25], [37], eye gaze [21], [34], hand joints [22], [35], and facial expression [24], [38]. These are available to developers through APIs, as well as captured by ALVR [2] in the BEHAVR setup. We follow the data structure definitions from the OpenXR standards [20]. The main elements of the data structures are *position*, *rotation*, and *linear* and *angular velocities*. Position, and linear and angular velocities are expressed in  $x$ ,  $y$ , and  $z$  values of the Cartesian right-handed

coordinate system, and rotation is expressed in  $x$ ,  $y$ ,  $z$ , and  $w$  values of the Quaternion coordinate system.

**Body Motion (BM).** BEHAVR captures the position, rotation, and linear and angular velocities of body motion. The four elements are captured for both of the left and right controllers (13 values per controller), whereas only the position and rotation are captured for the headset (total 7 values) [25]. This sensor group has received much attention in prior work [31], [39], [40], [43], [62]. However, the focus was *only* on position and rotation values.

**Eye Gaze (EG).** BEHAVR captures the position and rotation of eye gaze for both left and right eyes (7 values per eye) [21], [58]. Some of the prior work has also looked into eye data, but from different angles [46], [56]. In [46], the authors analyzed eye gaze data together with body motion data. Meanwhile, [56] looked into eye parameters (*i.e.*, pupil size and eye openness). In BEHAVR, we analyze eye gaze as an independent sensor group (see Section 4.1.3).

**Hand Joints (HJ).** The OpenXR standard tracks the motion of each hand as a composition of 26 *individually articulated joints* (see data structure `XrHandJointEXT` in [23]). BEHAVR captures the position and rotation of each joint [22] with a total of 182 values for all joints in each hand.

**Facial Expression (FE).** The OpenXR standard tracks 63 facial elements (defined in the data structure `XrFaceExpressionFB` [24]). Thus, 63 facial element values can then be mapped to 31 Action Units (AUs) as per the Facial Action Coding System (FACS) [12]. Each AU in the FACS standard represents one facial muscle movement. The combinations of AUs may correspond to a particular emotion. For example, the combination of AU6 (Cheek Raiser) and AU12 (Lip Corner Puller) may indicate a person smiling, which can be correlated with the emotion happiness or joy [15].

The BM sensor group exists in every VR device which supports basic VR functionality. While eye gaze tracking has been supported by other headsets (*e.g.*, HTC Vive [46], [56]) for a while, Meta made it available recently together with FE tracking on Quest Pro that was released in November 2022 to enable more realistic avatars [34], [38]. To the best of our knowledge, we are the first to study the HJ and FE sensor groups for user identification.

### 2.3. VR Sensor Data in Privacy Policies

Privacy laws, such as the GDPR [14] and CCPA [49], require disclosure of data collection, use and sharing practices. Both CCPA (in §1798.140(c)) and GDPR (Article 4(14)) define *behavioural characteristics* as part of “biometric information” or “biometric data” that can uniquely identify a person. This motivates us to take a closer look at real-world VR apps and platforms and see what they disclose about VR sensor data in their privacy policies.

We look at the top 100 apps from the “Most played VR games” list on Steam [52] and download their privacy policies. As of May 2023, only 60 apps provided a privacy policy. We read those privacy policies and use ChatGPT to understand how they disclose the collection of VR sensor data. More specifically, we look for statements on “biometric data” or “sensory data”, as well as more specific types (*e.g.*, “head movement”) in any of the sections; only a few (9 out of 60) privacy policies discuss the collection of VR sensor data, and some make conflicting statements.

These observations are aligned with the findings in [57], that many VR apps did not provide a privacy policy or did not disclose VR sensory data collection adequately. On the other hand, Meta, the maker of Quest Pro, indicates in its privacy policy that they collect data and use it for personalization [27]. This further motivates us to study the extent of how real-world VR apps and VR platforms can uniquely identify users based on their activity in VR.

### 2.4. Threat Model

We consider a passive (*honest-but-curious* [45]) adversary, whose goal is to identify users from VR sensor data. In the training phase, the adversary observes users’ activities in VR apps, captures, processes the sensor data streams generated by the users, and trains models for classifying blocks of sensor data for each user. In the testing phase, the adversary observes another sensor data stream and applies the trained models to decide which user generated it.<sup>2</sup> We distinguish two types of adversaries, depending on their vantage points and how much/which app’s sensor data they have access to, described next and depicted in “①” in Fig. 2.

**App Adversary.** The app adversary ( $adv_{app}$ ) has access to sensor data collected from APIs available within a single app. This mimics an app developer or any third party that has the same permissions or receives the data from the app. It corresponds to the client adversary in the taxonomy in [18] and has been previously studied for identification within a single app, *e.g.*, using a large dataset from Beat Saber [43] or collecting data from custom apps [39], [42], [56].

**Device Adversary.** The device adversary ( $adv_{dev}$ ) has access to all sensor data collected from all VR apps running on the device, and corresponds to the hardware adversary in the taxonomy in [18]. Its capabilities are available to

2. We consider a fixed set of users we train and test on:  $u_1, u_2, \dots, u_n$ . We do not classify users we have not trained on although that can be studied using the confidence of the classifier in future work.

the VR device (*e.g.*, Quest Pro) and its operating system, as well as to the PC in our SteamVR setup; furthermore, a compromised library with functionality similar to ALVR that reads the sensor data stream, could act as the device adversary. To the best of our knowledge, this device adversary has not been studied for user identification in VR, primarily because collecting and observing sensor data across multiple real-world apps were not previously possible.

Both adversaries collect users’ sensor data trace  $D$  from the four sensor groups discussed in Section 2.2. Both train models to identify a user  $u_i$  among a group of  $n$  users ( $u_1, \dots, u_n$ ), whose data can be observed. Their main difference is while the app adversary has access to data from one app (*e.g.*,  $a_j$ ), the device adversary can have access to data from all apps on the device. Both adversaries train one model per sensor group, which predict the label for each sensor data block and can combine all labels of blocks through max voting per user [10]. Furthermore, the device adversary can decide to train on data from all apps, or groups of similar apps as defined in Section 2.1. See Section 4.2 and 5 for details on the models<sup>3</sup> and their evaluation.

## 3. Experimental Setup & Data Collection

### 3.1. Using ALVR as a Vantage Point

In our data collection, we use the latest VR device from Meta, Quest Pro – the state-of-the-art VR device that was released in Nov. 2022. While other VR devices also work with SteamVR [60], Quest Pro collects eye gaze and facial expression data [34], [38], in addition to body motion and hand joints data [35], which have been collected by older VR devices such as *e.g.*, Meta Quest 2.

The BEHAVR data collection system is depicted in “①” in Fig. 2. Although the Oculus OSon Quest Pro can natively run VR apps, we use the SteamVR setup [60] that allows us to intercept and record sensor data. In BEHAVR, Quest Pro sends sensor data to a PC that runs a VR app and the Quest Pro and PC are connected via WiFi. BEHAVR integrates the ALVR [2], open-source software that can run VR apps on a PC. With the help of SteamVR, ALVR can run Steam apps that provide VR support on Quest Pro: the sensor data sent from Quest Pro are received by ALVR and become input to the app to process and render the app’s VR environment in real-time. Finally, the app sends the rendering results back to the Quest Pro, so the headset displays the VR environment to the user.

While, the SteamVR setup was intended to enhance VR performance, by performing heavy tasks on the PC, we use it for passive data monitoring, for the first time. This setup allows us to instrument parts of ALVR’s source code that receive sensor data from the Quest Pro and save the data as time series for all four sensor groups. It enables BEHAVR to collect sensor data for many real-world apps, which was

3. We use the terms “adversary” and “model” interchangeably. For example, a BM device adversary uses an identification model, trained and tested on body motion data from all apps on the device.

not previously possible: prior work had to develop custom apps/specific tasks for specific research purposes.

### 3.2. User Study & Data Collection

We conducted an IRB-approved user-study (IRB #2848). We recruited 20 participants from the age group of 20-40 years old, which is representing of the majority of VR users [5]. The data collection was performed by three authors. We spent approx. 5 – 6 hours (including briefing and training) to collect data for 20 real-world apps for one user, over a period of approx. 3 months in total for 20 users.

Each user was asked to wear a Quest Pro headset, hold the controllers, and interact with all 20 apps in our corpus. For each app, the user was asked to complete an app-specific activity, whose duration was typically up to 3 minutes; see Table 4 in Appendix A. A research team member provided rough prompts to the VR user during their user-app interaction. For example, in Beat Saber, our team member would instruct the user: “Please complete the tutorial once, then put down the controllers and complete the tutorial one more time with bare hands”. Meanwhile, BEHAVR (*i.e.*, the instrumented version of ALVR) was running and recording sensor data from Quest Pro. For each app, a user was requested to complete the app-specific activity twice and collect two sensor data traces: the first for model training and validation, and the second for evaluation. The BEHAVR dataset consists of all traces, including all data from four sensor groups from two sessions per user per app, from all 20 users.

**Discussion.** The size of our participant pool aligns with that of similar prior studies that required involved user participation (*e.g.*, [31], [40], [42], [46], [56]), that considered up to 16-50 participants. Differences include the following. First, most studies asked the participants to perform a limited set of tasks in custom apps, which are designed to elicit specific behavior that lends itself to identifiability, thus termed as “adversarial VR” *e.g.*, in [42]; in contrast, we ask users to perform generic tasks, natural to the real-world apps. Second, we observe user behavior in real-world apps. [39] considers hundreds of users, but they were asked to perform simple tasks, which are not comparable to those in real-world apps. In [43], the authors also considered a popular real-world app (Beat Saber) and a large number (50K) users from an existing dataset (provided by BeatLeader [47]) and one sensor group (body motion data). Datasets with this number of users are impossible to collect from in-person user studies. The focus of BEHAVR is to provide a framework to scale in two dimensions beyond just the number of users (as depicted in Fig. 1): new sensor groups, and the number of (real-world) apps. Future work could leverage/combine the scale of automatically collected and provided datasets, with the richness of user studies.

## 4. Data Analysis and Model Training

This section presents the BEHAVR pipeline for processing the sensor data (Section 4.1, also see “②” in Fig. 2) and

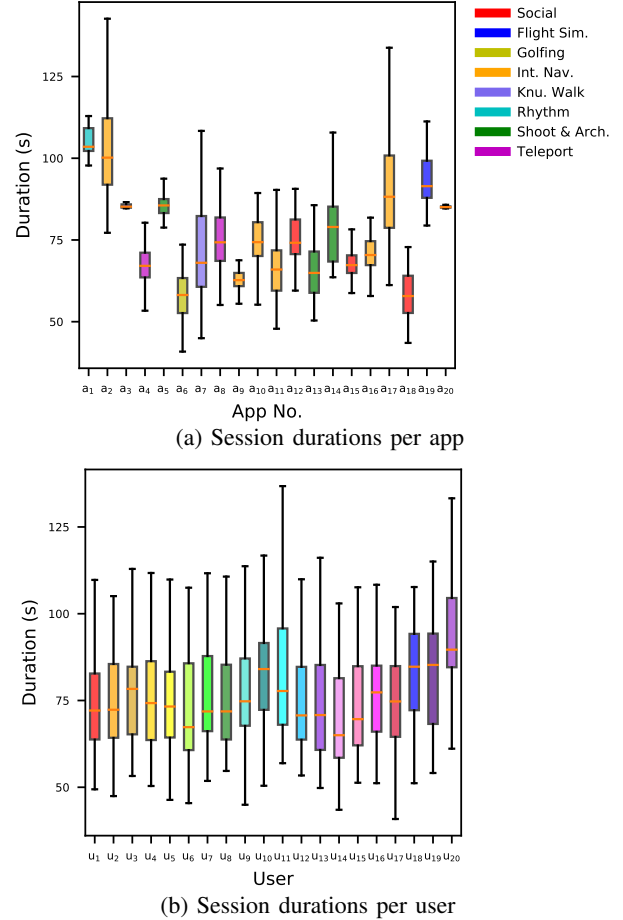


Figure 3: Session durations: There are 20 users and each interacts with 20 apps (colors represent app groups).

for model training (Section 4.2, also see “③” in Fig. 2) .

### 4.1. Sensor Data Summarization

In this part, we convert the sensor data streams (in BEHAVR dataset) into feature vectors, which are suitable for a non-sequential model (*e.g.*, Random Forest). There are three steps: data analysis, processing, and feature engineering, as discussed next.

**4.1.1. Insight: Variability.** The BEHAVR dataset exhibits variability across users, apps, and sensors, even when we give all users the same prompts then they perform the same tasks. Allowing or designing for variability was a decision we made on purpose, to capture real users’ behavior. From a *user* perspective, the user has the freedom on how, and at what pace, to perform the activity in each app. For example, in  $a_{10}$  (an interactive navigation app), we give a prompt to the user: “Look around first”; user has the freedom to turn left or right to look around the room. In  $a_{18}$  (a social app), a user is first instructed to approach a mirror and then instructed to: “Say hi to your avatar”. Users typically greet the avatar by waving one or both hands and

moving their bodies. From the *app* perspective, variability is caused by different apps having different prompt sets, which results in different session durations across different apps. Furthermore, each user may complete the same set of prompts for an app in different durations as they are asked to complete two sessions per app. From the *sensor* perspective, variability occurs as the four sensor groups operate with different sampling rates and time spans, *e.g.*, hand joints sensor data have less data points than other sensor groups, during the same tasks, because we usually ask users to use bare hands only in the middle of the interaction with an app. We focus on the variability in *session durations* across users and apps. To illustrate that, we plot the distribution of session durations per app (see Fig. 3a) and per user (see Fig. 3b). In Fig. 3a, we observe that different users interact with the same app in different durations: the average durations vary across apps, but the variance of duration for each app is relatively small. Conversely, in Fig. 3b we see the users’ session durations across apps: the average durations are closer to each other, but have larger variance each user. Furthermore, each sensor group has its own collection duration. Based on these observations, we summarize the sensor data on per app and per sensor group basis.

#### 4.1.2. Data Processing.

Next, we describe data processing.

**Pre-processing.** This step aims to obtain valid time series data with unique timestamps. First, we de-duplicate timestamps and delete invalid columns (*e.g.*, columns with only zeros). Next, we check any data corruption (*e.g.*, rows that contain error messages) and replace the invalid values using neighboring rows.

**Block Division.** The goal of this step is to process the sensor data streams by dividing them into time blocks, and summarizing each as a feature vector, to be used later for model training. One challenge is how to choose the length of this block. For block division, we first experimented with a fixed-block length (which we refer to as FBL) approach, which has also been used in [39]. FBL divides time series data into blocks, in which each block has a fixed length (*e.g.*, 1 or 2 seconds), and it ignores the variability of users, apps, and sensors. Since there is much variability in the BEHAVR dataset, FBL does not work well in our case. Thus, we develop an intuitive but robust method, which we refer to as *fixed-block amount* (or FBA), guided by previous observations on variability across apps and users. FBA divides the time series into a fixed number (amount) of blocks for each sensor group and each app; this is instead of using blocks with a fixed length. We implement the method on the whole dataset, which includes time series data from the four sensor groups (see Section 2.2).

Fig. 4 shows an example of applying FBA to the BM sensor group; it illustrates how we process one value, *i.e.*,  $x$  of the headset rotation for one app  $a_j$ . We consider the time series data related to this value, and decide in how many blocks we divide the time series into. In this example, we consider one app  $a_1$  and three users, namely  $u_1, u_2, u_3$ , whose session durations are 3.6 sec, 4.1 sec, 4.6 sec, respectively. We compute the average duration for

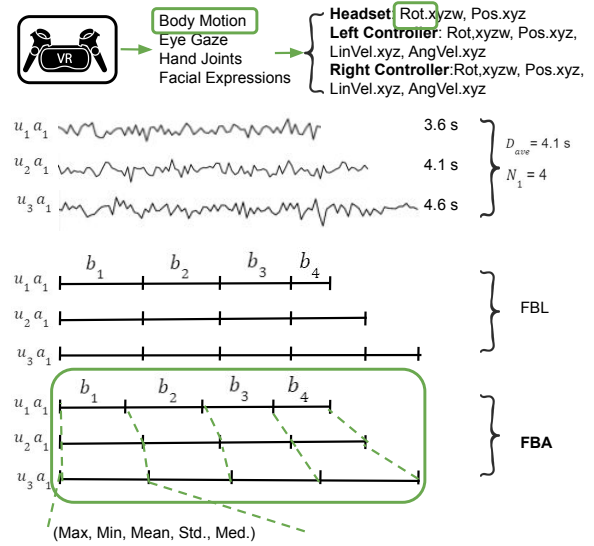


Figure 4: FBA illustration for the  $x$  value of headset rotation from the BM sensor group.

each app; for  $a_1$ , this is  $\sum (3.6 + 4.1 + 4.6)/3 = 4.1$  sec. Then we define its floor as  $N_1 = \lfloor 4.1 \rfloor = 4$ , and we divide the timeseries of each user into  $N_1 = 4$  blocks, each block with duration close to 1 sec. In order to be able to divide the timeseries in more or less number of blocks, with much shorter or longer duration than 1 sec accordingly, we introduce another parameter  $r \in (0, 2]$ , which controls the final amount of blocks (“final block amount”) for each app  $a_j$ :  $N_{FBA_j} = r \cdot N_j$ . When we increase the ratio  $r$ , we increase the final block amount while decreasing the block length (amount of time per block). The key insight here is, unlike FBL, FBA takes into account the variability across users to scale the number of blocks for each app,  $N_{FBA_j}$ , so as to align similar user-app interactions in the time series.

**Summarization.** We summarize the information in the time-series of each block with a vector of 5 statistics, *i.e.*, maximum, minimum, mean, standard deviation, and median within each block, which will serve as features next. This summarization was originally proposed in [39] for body motion data and was also used in [43].

**Block Post-Processing.** In this step, we take the table of blocks x features produced in the previous steps, and we check the data validity, first by blocks (rows), then by features (columns). First, we remove invalid blocks (*e.g.*, BM data contain many zeros when a user uses bare hands), and we approximate missing values (*e.g.*, in HJ data, we replace missing median values with mean values). Then, we delete unwanted features from each block, *e.g.*, features with all zero/one values or irrelevant to classification task.

**4.1.3. Feature Engineering.** After the previous steps, we further select and augment the features, as follows.

**Body Motion.** We use all features, similarly to [39], [43].  
**Eye Gaze.** We have 30 features after post-processing, and we augment with 16 more as follows. Prior work has shown

that IPD (*i.e.*, the  $y$  positional distance between the left and right eyes) can be used to profile VR users (*e.g.*, gender identification [42]). If  $f_L$  and  $f_R$  are the positional/rotational features for left and right eyes, we also include their distance,  $f_{(LR)}^a = abs(f_L - f_R)$ , as a feature.

**Hand Joints.** We choose top  $\sim 500$  features using the feature importance technique [32] for model input. As most users interact with apps using their dominant (*i.e.*, either left or right) hand, we do not explore feature augmentation by correlating the left and right hands’ HJ features.

**Facial Expression.** First, we use all features from block post-processing; see Table 5 in Appendix B.1. In addition, we look into an identification based on AU combinations representing an emotion, *e.g.*, AU6 and AU12 represent happiness. We perform feature selection and we use only specific features that represent emotion [15] to train and evaluate the model. For example, if the adversary aims to identify a user based on happiness, they choose elements (5, 6) and (33, 34) corresponding to AU6 and AU12 to train/evaluate the model; thus, the total number of features is  $(5, 6, 33, 34) \times (5 \text{ statistics}) = 20$ . Finally, we combine all AUs representing emotions (*i.e.*, 125 features corresponding to all emotions) to train and evaluate models.

**Final Features.** After completing data analysis, processing, and feature engineering, we obtain the final summarized data for each of the four sensor groups, as summarized in Table 5 in Appendix B.1. These final features serve as input to training the adversary’s models, described next.

## 4.2. User Identification Models

**Classification Task.** For each block, we perform a multi-class classification task, where the classifier’s goal is to uniquely identify user  $u_i$  among the set of  $n$  (*i.e.*, 20) users within-app for an app adversary model, or across apps for a device adversary model (see Section 2.4).

**Train-Test Split.** We gathered sensor data from users in two sessions per app, each involving completing the same app-specific activity (see Section 3.2). Data from the first session are split 90% for training ( $D_{train}$ ) and 10% for validation ( $D_{val}$ ), while data from the second session is utilized to evaluate the model performance.

**Model Architecture.** We explored models including Random Forest (RF) [30], Gradient Boosting (XGB) [16], Support Vector Machine (SVM) [8], and Long Short-Term Memory Networks (LSTM) [26]. We found that RF and (for several apps) XGB performed best on the BEHAVR dataset; this aligns with the closest prior work [39]. More details on algorithm selection can be found in Appendix B.2.

**Hyperparameters Tuning.** In BEHAVR, for RF, first we tune hyperparameters by varying  $n$ -estimators and  $max$ -depth from (50, 200) and (1, 20) respectively in five iterations. Then, we select the best model based on five-fold cross-validation. Finally, based on the accuracy obtained from the primary analysis, we choose the optimal point of FBA ratio  $r$ : our evaluations rely on this final model. Additional information is available in Appendix B.1.

**Model Training** We use the FBA method to divide each session into  $N_{FBA_j}$  blocks per user in an app  $a_j$ , *i.e.*,  $[b_1, b_2, \dots, b_{N_{FBA_j}}]$ . The total time length per session per user is  $T$ , and each block’s time length is  $t$ . We use all blocks from  $D_{train}$  from the first session for training. For evaluation, we pick  $s$  number of blocks per user;  $s$  represents a *sub-session* that has  $[b_1, b_2, \dots, b_s]$  blocks, where  $s \leq N_{FBA_j}$ . The total time  $S_t$  for the sub-session is  $s \times t$ .  $S_t$  allows us to investigate the minimum time we need per sensor group per user for identification. The sub-session becomes the whole evaluation session per user when  $s = N_{FBA_j}$  and  $S_t = T$ . Finally, we perform a classification task for each block (*i.e.*, predict the label for each  $b_1, b_2, \dots, b_s$ ) and use maximum voting [10] across all blocks to determine the final label for each user.

**Different Adversaries and Their Models.** In Section 2.4, we described our adversaries, which only differ in their vantage point, which determines what data they have access to and can use to train and evaluate models. The app adversary trains an *app model* on each app’s data. The device adversary has access to all data on the device. It can choose to train a *universal model* that uses data from all apps ( $a_1, \dots, a_{20}$ ); or it can choose to train on a subset – a *group model* for an app group the reasons outlined in Section 2.1.

Suppose an app group (*e.g.*, social or flight simulation apps) has  $n_g$  number of apps. The device adversary trains an app group model on all  $n_g$  apps’ training data. First, we consider the scenario where the adversary attacks an app in that group it has already trained on: the adversary can apply the model on each app’s test data to identify users. In addition, we identify users across different  $n_g$  apps by evaluating the app group model with an average amount of test data from all apps (*e.g.*, with 3 apps in a group, we use 33.33% sub-session time from each app for evaluation) which is going to refer as *average data* or  $a_{avg}$ ; this variation is to make a fair comparison using the same amount of data for evaluation. Second, we consider a *zero-day-app* scenario, where the adversary attempts to identify a user from an app that it has not previously trained on. To that end, we train an app group model with  $n_g - 1$  apps’ training data and test on  $n_g^{th}$  app ( $n_g^{th}$  app’s data is not in  $D_{train}$ ). Finally, we evaluate each group model on any randomly selected app from different groups.

**Top Features.** For each model, we analyze the feature importance for RF and XGB using information gain [32]. This mimics an adversary who wants to minimize its work.

## 5. Evaluation Results

In this section, we evaluate the performance of BEHAVR’s app and device models for user identification. Table 2 summarizes the results. For each sensor group (in Sections 5.1, 5.2, 5.3, and 5.4), we evaluate 20 app models (*i.e.*, one model for each app), as well as the device model, guided by the following research questions (RQ):

- **RQ1 (Accuracy):** How well can a user be identified using VR sensor data from a particular sensor group? How do these groups compare to each other?



TABLE 2: Identification accuracy (in percent) for app adversary ( $adv_{app}$ ) and device adversary ( $adv_{dev}$ ) w.r.t. sensor groups. The **app adversary** ( $adv_{app}$ ) trains and evaluates an app model on sensors data from a single app (listed in **App No** column). The **device adversary** ( $adv_{dev}$ ) has two rows. The first row (e.g.,  $a_{12}, a_{15}, a_{18}$ ) reports results from  $adv_{dev}$  training a group model on all apps in that group and evaluating on each individual app. The second row for  $adv_{dev}$  reports results from training a group model and evaluating on average data of that group (e.g.,  $a_{avg}$  means that each app contributes to 33.33% of the data if  $n_g = 3$ ). Each of golfing, rhythm, and knuckle-walking groups contains exactly one app; thus,  $adv_{app}$  and  $adv_{dev}$  are the same (filled with “both” in **Adver.** column).

App Group	Adver.	App No.	Sensor Group			
			BM	EG	HJ	FE
Social	$adv_{app}$	$a_{12}, a_{15}, a_{18}$	85, 95, 95	80, 90, 85	60, 65, 75	95, 100, 100
	$adv_{dev}$	$a_{12}, a_{15}, a_{18}$	95, 95, 95	75, 90, 85	70, 85, 75	100, 100, 100
	$adv_{dev}$	$a_{avg}$	100	95	90	100
Flight Sim.	$adv_{app}$	$a_3, a_{19}, a_{20}$	95, 100, 95	85, 90, 75	80, 75, 75	100, 95, 95
	$adv_{dev}$	$a_3, a_{19}, a_{20}$	95, 100, 100	90, 90, 90	80, 80, 75	100, 100, 95
	$adv_{dev}$	$a_{avg}$	100	95	95	100
Interactive Navigation	$adv_{app}$	$a_2, a_9, a_{10}, a_{11}, a_{16}, a_{17}$	95, 80, 95, 95, 95, 100	80, 80, 85, 95, 75, 80	60, 40, 60, 60, 70, 90	100, 100, 90, 95, 100, 100
	$adv_{dev}$	$a_2, a_9, a_{10}, a_{11}, a_{16}, a_{17}$	95, 85, 90, 95, 95, 100	75, 60, 80, 80, 60, 75	55, 40, 60, 75, 75, 90	100, 100, 95, 100, 100, 100
	$adv_{dev}$	$a_{avg}$	100	95	85	100
Shooting & Archery	$adv_{app}$	$a_5, a_{13}, a_{14}$	95, 90, 100	85, 75, 90	70, 40, 80	90, 100, 100
	$adv_{dev}$	$a_5, a_{13}, a_{14}$	95, 100, 100	85, 80, 90	70, 55, 80	90, 100, 100
	$adv_{dev}$	$a_{avg}$	100	90	85	100
Teleport.	$adv_{app}$	$a_4, a_8$	70, 80	90, 70	35, 45	95, 95
	$adv_{dev}$	$a_4, a_8$	75, 90	90, 75	35, 50	100, 95
	$adv_{dev}$	$a_{avg}$	85	90	50	100
Golfing	both	$a_6$	80	70	50	90
Rhythm	both	$a_1$	100	95	75	100
Knu.-walk.	both	$a_7$	95	80	65	100
All	$adv_{dev}$	$a_1, a_2, \dots, a_{20}$	90 – 100	50 – 80	45 – 95	100
	$adv_{dev}$	$a_{avg}$	100	90	100	100

- *RQ2 (Sub-session Time  $S_t$ ):* How long does it take to identify a user?
- *RQ3 (Top Features):* What are the top features for identification?

In Section 5.5, we also evaluate the app-group models, discussed in Sections 2.1 and 4.2, answering the following:

- *RQ4 (App Groups):* Can we identify a user within a group of similar apps? What if the app is *not* included in the training of the adversary’s model (zero-day-app scenario)?
- *RQ5 (Important Sensor Groups):* What are the most important sensor groups in general, and as they relate to particular app groups?

## 5.1. Body Motion Models Evaluation

*RQ1 (Accuracy).* The identification accuracy for body motion app models is 100% in 3 apps and  $\geq 95\%$  (i.e., at most 1 out of 20 user is falsely identified) in 14 apps (see  $adv_{app}$  results from BM column of Table 2). These findings align with results in prior work (see Section 6). Most apps, such as Beat Saber ( $a_1$ ; extensively studied in [43]), archery ( $a_5$ ), and shooting ( $a_{13}$ ), demand significant body motion (headset and controllers movement). Other apps that require less body motion (e.g.,  $a_4$  and  $a_8$ , in which users perform teleportation to move around) provide  $\sim 70\%$  accuracy. For the device model, the identification accuracy is 100% as the device adversary considers a larger amount of data and tasks for training (see  $adv_{dev}$  BM column of Table 2).

*RQ2 (Sub-session Time  $S_t$ ).* For the app models, identification accuracy is  $\sim 80\%$  considering 4s sub-session time ( $S_t$ ) per user on average. The app models require at least 16s of  $S_t$  to reach 90% identification accuracy (see Fig. 7a in Appendix C.1). The device model gives higher accuracy with similar  $S_t$ , because it is trained with all data from 20 apps (see Fig. 7e in Appendix C.1). Thus, it accumulates the knowledge of the user behavior across all apps.

*RQ3 (Top Features).* In Appendix C.2, Table 7 presents the top-3 features for user identification using app models. For the *app model*, the top features are influenced by app-specific activity; for example, in social apps ( $a_{15}, a_{18}$ ) users mostly walk, making the  $y$ -position of the headset (height) the top feature. In contrast, flight apps ( $a_{19}, a_3$ ) require that users are sitting down and make left-right head movements for airplane control; thus, top features are obtained from the headset’s  $x$ -position (left-right movements). Other apps that require both head and controller movement, such as archery ( $a_5$ ) and knuckle-walking ( $a_7$ ), have the movement/velocity of the headset and controllers as top features. For the *device model*, the  $y$ -position of the headset is a top feature; see Fig. 8a in Appendix C.2. The next most important feature is the  $z$ -position of the headset, which represents the horizontal (forward-backward) range of the user’s head movement. Fig. 9a in Appendix C.2 shows the importance of headset features: identification accuracy improvement, compared to controller features alone, is within 5% to 35% ( $\sim 21\%$  on average) across all apps.

**Key Takeaways.** In general, user identification with BM is influenced by app-specific activity (app adversary) and user-specific features (device adversary). Height holds importance in both app (where app-specific activities are height-related, *e.g.*, walking) and device models, whereas horizontal/vertical head movements are related to app activities.

## 5.2. Eye Gaze Models Evaluation

*RQ1 (Accuracy).* App models provide  $\geq 90\%$  accuracy for 8 apps and  $\geq 85\%$  for 12 apps. The remaining apps have  $\geq 75\%$  accuracy. We observe that the identification accuracy is influenced by frequent object-eye interaction, *e.g.*, Beat Saber ( $a_1$ ) model gives 95% accuracy as users frequently look at and follow the movement of virtual objects in this app. Similarly, archery, shooting, and flight simulation app models show high identification accuracy due to frequent eye-object interaction. The device model’s accuracy can be up to 100% (see EG column in Table 2).

*RQ2 (Sub-session Time  $S_t$ ).* For the app models, the accuracy is  $\sim 50\%$  when we consider at least 5s of sub-session time per user on average. The accuracy increases to  $\sim 70\%$  when we consider at least 19s of sub-session time per user (accuracy may vary depending on apps, see Fig. 7b in Appendix C.1). For the device model, Fig. 7e in Appendix C.1 shows that 80% accuracy can be achieved by considering at least 17s of sub-session time.

*RQ3 (Top Features).* For both app and device models, Table 7 in Appendix C.2 and Fig. 8b in Appendix C.2 show that augmented features contribute the most to user identification with eye gaze data. The top features are the  $y$ -rotation that correlates left and right eyes (*i.e.*, “Quat.y Left Right”) for app adversary and IPD for device adversary. This matches the intuition that inspires us to use the feature augmentation technique for eye gaze (*i.e.*,  $f_{LR}^a$ ) in the first place. Fig. 9b in Appendix C.2 shows that features from the augmentation technique improve model accuracy significantly (5–35% or  $\sim 20\%$  on average) across all apps.

**Key Takeaways.** Augmenting the standard features with the distance between the eyes improves identification accuracy.

## 5.3. Hand Joints Models Evaluation

*RQ1 (Accuracy).* The app models provide  $\geq 70\%$  identification accuracy for 9 apps, which involve diverse hand movements and gestures (see Table 4). For example, in  $a_1$  (Beat Saber), users swing light sabers to cut blocks using both hands; in  $a_5$  (archery), users repetitively shoot arrows with a bow. For  $a_{17}$  (chess), users grab and move chess pieces by hand, highlighting the significance of hand joints as a sensor group. Conversely, teleportation ( $a_4$ ,  $a_8$ ) provides the lowest accuracy ( $\sim 35\%$ ) as they require much less hand movements. For the device model, the accuracy is mostly  $\geq 85\%$ . This is consistent with the body motion device model results: *i.e.*, the device model outperforms app models in terms of accuracy (see HJ column of Table 2).

*RQ2 (Sub-session Time  $S_t$ ).* For the app models, the accuracy is up to 60% or higher when considering  $S_t$  of at least 20s (see Fig. 7c in Appendix C.1). For the device model, by considering at least 120s of  $S_t$ , the model provides 90% accuracy (see Fig. 7f in Appendix C.1).

*RQ3 (Top Features).* For the app models, Table 7 in Appendix C.2 shows that the top features are influenced by app-specific activities.<sup>4</sup> For example, the top features for  $a_1$  (Beat Saber) are the positions of joints 1 and 3 (*i.e.*, thumb metacarpal and palm) of the right hand and joint 24 (little intermediate) of the left hand. Intuitively, these joints are actively exercised when making a fist for holding light sabers. Next, in  $a_{17}$  (chess), joints 22 and 25 (*i.e.*, little metacarpal and distal) of the right hand (that most people use for moving chess pieces) are listed as top features. For the device model (see Fig. 8c in Appendix C.2), the top features are the positions of left-hand joints 1 (palm), 2 (wrist), 6 (thumb distal), 7 (index metacarpal), and right-hand joints 1 (palm), 2 (wrist), 4 (thumb proximal), and 5 (thumb distal). In general, they represent a user’s natural hand movements and gestures (*e.g.*, making an open fist, grabbing, waving, etc.). For left and right hands, the dominant features are joint positions and/or rotations, respectively as users tend to position their left hand naturally while using their right hand for app-specific activities. Fig. 9c shows that identification accuracy decreases by  $\sim 10\%$  on average if right-hand features are not considered.

**Key Takeaways.** Identification using hand joints data takes into account natural joint positions (left hand) and app-specific hand gestures (right hand).

## 5.4. Facial Expression Models Evaluation

*RQ1 (Accuracy).* The app models provide  $\geq 95\%$  accuracy for 17 out of 20 apps and 90% for the remaining 3: facial expression is highly effective for user identification. The device model achieves up to 100% accuracy, consistent with other sensor groups (see FE column of Table 2).

*RQ2 (Sub-session Time  $S_t$ ).* For the app models, most provide  $\geq 85\%$  accuracy with  $S_t$  of only 5s, and  $\geq 90\%$  accuracy with 18s (see Fig. 7d in Appendix C.1). The device model can identify a user uniquely with 95% with just 3s and 100% accuracy within 17s (see Fig. 7e in Appendix C.1); demonstrating the high effectiveness of FE.

*RQ3 (Top Features).* For the app models, the top-3 features for each app are listed in Table 7 in Appendix C.2.<sup>5</sup> We can correlate facial elements to the app-specific activities (*e.g.*, in  $a_9$ : job simulation, users eat a donut; this correlates with element 27—jaw movement as a top feature) and valence/arousal states (*e.g.*, social, rhythm: elements 5 and 6, which correspond to AU6 is action unit for happiness).

For the device model (see Fig. 8d in Appendix C.2), top features include elements 5, 6, 25, 28, and 51, *i.e.*, cheek

4. See [22] for the descriptions of the joints—these joints are numbered from 1 – 26 in this paper, instead of 0 – 25.

5. See [15], [24] for descriptions – these elements are numbered from 1 – 63 in this paper, instead of 0 – 62.

TABLE 3: Identification accuracy (in %) based on combinations of AUs that represent emotions w.r.t. app groups; *Emotional States*, *A/V=Arousal/Valence*: LA = low arousal, HA = high arousal, PV = positive valence, NV = negative valence

Emotion	A/V	Identification accuracy (%) in App Groups									
		Social		Flight Sim.		Int. Nav.		K.-walk.	Rhy.	Shooting	Archery
		$a_{18}$	$a_{15}$	$a_{19}$	$a_{20}$	$a_{16}$	$a_{10}$	$a_7$	$a_1$	$a_{14}$	$a_5$
Happiness	HA/PV	100.0	100.0	80.0	75.0	80.0	75.0	100.0	95.0	80.0	75.0
Surprise	LA/PV	100.0	95.0	80.0	80.0	75.0	85.0	100.0	100.0	90.0	85.0
Anger	HA/NV	95.0	95.0	95.0	85.0	85.0	85.0	90.0	95.0	90.0	85.0
Disgust	HA/NV	75.0	75.0	65.0	55.0	60.0	75.0	70.0	70.0	75.0	75.0
Fear	LA/NV	90.0	100.0	85.0	90.0	80.0	95.0	100.0	100.0	95.0	90.0
Sadness	LA/NV	95.0	90.0	100.0	90.0	80.0	80.0	90.0	90.0	95.0	85.0
All Emotion AUs	All	95.0	100.0	95.0	90.0	95.0	90.0	100.0	100.0	100.0	85.0
All AUs	All	95.0	100.0	100.0	95.0	100.0	90.0	100.0	100.0	100.0	90.0

raiser, jaw drop, jaw thrust, and lips toward respectively. We observe that both emotions and natural expressions are key features for user identification in the device model, *e.g.*, element 5 is part of user expression when feeling joy; elements 28 and 51 are parts of natural expressions representing the outward movement of the lower lip and opening movement of the lips.

**5.4.1. Facial Emotion Models Evaluation.** In this section, we focus specifically on facial elements/AU combinations that represent an emotion (see descriptions in [15], [24] and results in Table 3), rather than all/other facial expression. We argue that arousal/valence states in VR may induce certain emotions, similar to what happens in the real world. For example, socializing, whether in-person or virtually, can make a person happy (HA/PV), or seeing a positive/new environment can induce joy/surprise (positive valence). From Table 1, we pick one or two apps from seven groups, representing the rest of the apps and groups.

The results confirm our hypothesis that facial elements/AUs indicating emotions can be used for user identification, correlating strongly with the app’s arousal/valence states. Social apps’ models use AU combinations that represent happiness and surprise and provide  $\geq 95\%$  accuracy. For flight simulation or shooting apps, which have mostly negative valence, combinations that represent happiness may not give high accuracy in user identification; ie apps  $a_{14}$  (shooting) and  $a_{20}$  (flight simulation), give 80% and 75% accuracies, respectively, when identifying a user based on facial elements/AUs of happiness. Contrarily, both apps provide  $\geq 90\%$  accuracy based on facial elements/AUs representing fear. Furthermore, in some apps, app-specific activities and arousal/valence states may induce a mixture of emotions. For instance, in Beat Saber ( $a_1$ ), users may experience happiness due to the music/beat, fear from the tension of cutting blocks and avoiding obstacles at a fast pace, and even sadness or anger when missing some blocks. Consequently, the models for these apps achieve high identification accuracy by considering almost all emotions. In addition, the models for apps that have mostly neutral arousal/valence states (*e.g.*, interactive navigation apps) may not yield high accuracy ( $\sim 80\%$ ) for certain emotions with high arousals, such as happiness/sadness; as the VR environment/activity may not strongly induce any emotions in users.

Finally, combining all facial elements/AUs representing

emotions provides high accuracy across all apps (*i.e.*,  $\geq 90\%$  for most apps). Fig. 9d in Appendix C.2 shows that AU combinations representing emotions provide better identification accuracy compared to other facial expression AUs (that do not represent emotions) by 5 – 25% in most the apps (with some exceptions) and 5% on average. Specifically, considering positive/negative arousal/valence states for certain apps, accuracy improves with AU combinations that represent emotions, *i.e.*, by 25% for  $a_{20}$  (flight simulation) and 10% for  $a_{14}$  (shooting).

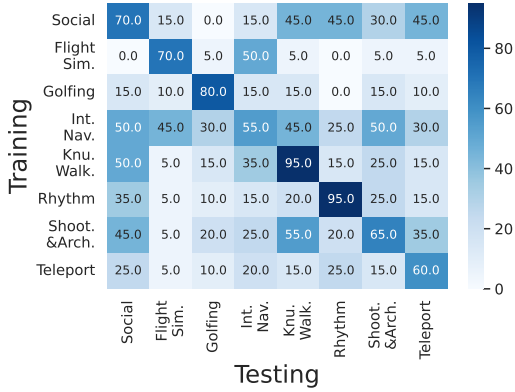
**Key Takeaways.** Our findings suggest that an adversary can select AU combinations that represent emotions w.r.t. the app’s arousal/valence state, to identify a user with low effort; *e.g.*, adversary can use a few facial features (*e.g.*, 20 for happiness in social apps) instead of all (*i.e.*, 325) facial features for adequate unique identification.

## 5.5. Comparative Evaluation

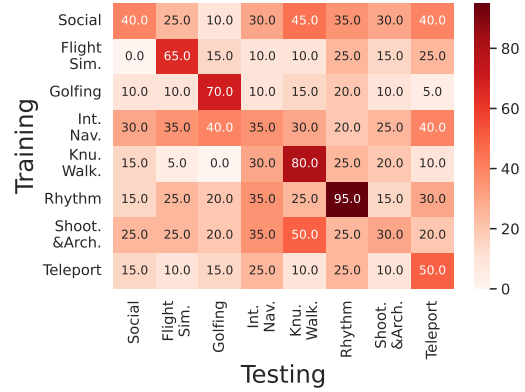
**5.5.1. User Identification across App Groups.** To address *RQ4*, we conduct experimental evaluation (see *adv<sub>dev</sub>* column in Table 2 for each group) on app groups described in Table 1. Additionally, we conduct evaluations for the *zero-day-app* scenario (see Fig. 5) defined in Section 4.2.

**Body Motion.** The performance of the *app group models* (trained on data from apps within an app group) and the *universal device model* (trained on all 20 apps) is comparable in terms of accuracy for BM, *e.g.*, both achieve up to 100% accuracy using averaged test data ( $a_{avg}$ ). We also see that the group models outperform the app models in general, which incentivizes the device adversary to opt for a group model over app models. For instance, in the shooting&archery group, the group model provides 10% higher accuracy for  $a_{13}$  compared to the app model. In the *zero-day* scenario, Fig. 5a shows that models evaluated on apps in the same group perform well (70 – 95% accuracy), while those tested on apps from different groups perform poorly (*i.e.*, 0 – 50% accuracy). This supports our hypothesis that group models are effective in the *zero-day-app* scenario.

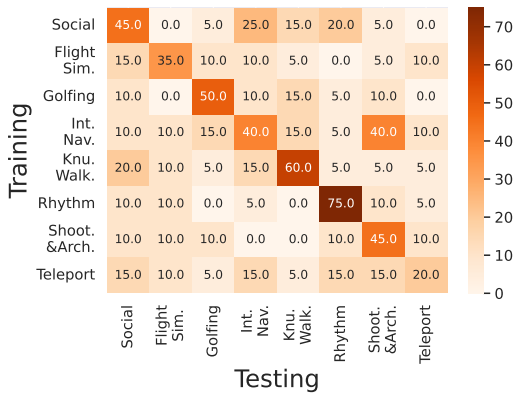
**Eye Gaze.** No app grouping based on eye gaze is observed due to the lack of specific activity. Table 2 indicates that group models perform similarly to app models. However, in the zero-day scenario, grouping can be valuable as within similar groups, there is a higher occurrence of eye-object



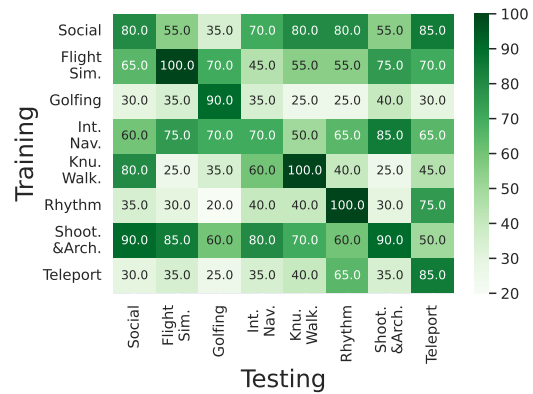
(a) Body Motion Sensor Group



(b) Eye Gaze Sensor Group



(c) Hand Joints Sensor Group



(d) Facial Expression Sensor Group

Figure 5: Identification accuracy (in percent) in the *zero-day-app* scenario. The adversary trains on the data from other apps in a group, and tests in a new app (for which it did not have training data) in the same group. The *diagonal* shows the accuracy for apps within the same group, whereas the *other values* show the accuracy for apps from other app groups.

interactions that potentially helps evaluate a new app without any training data. Fig. 5b shows a satisfactory diagonal in heatmap accuracy, supporting our claim.

**Hand Joints.** For hand joints, app group models and the universal device model have comparable performance, *e.g.*, using  $a_{avg}$ , the accuracy difference is within the range of 10–15% mostly. Akin to BM, HJ group models outperform the app models, *e.g.*, the social group model provides 20% higher accuracy for  $a_{15}$  than the app model. For most apps, the accuracy improvement is 5–10%. Fig. 5c shows the results for *zero-day-app* scenario. For HJ, mostly, a group model evaluated on its native apps provides higher accuracy (40–75%) than an app from different groups (~20%).

**Facial Expression.** For the facial expressions, both the app group models and the universal device model provide up to 100% accuracy. The group models exhibit similar or better performance than the app models; for many apps, this accuracy improvement is not significant (5%), since most app models for FE already have  $\geq 90\%$  accuracy. For the *zero-day-app* scenario, a model tested on apps from the same group provides higher accuracy (70–100%) than

apps from different groups (20–65% accuracy) for most of the cases (see Fig. 5d). However, several apps provide high accuracy within different groups for FE, *e.g.*, the social group model provides 80% accuracy on  $a_1$  and  $a_7$ , which share similar arousal/valence states (LA/PV, HA/PV) with social group. Additionally, the shoot&archery group model provides higher accuracy (*e.g.*, 85%) when tested on flight apps (*e.g.*,  $a_{20}$ ) as they share similar arousal/valence states (LA/NV, HA/NV) (see Table 1).

**5.5.2. Model Accuracy across Sensor Groups.** This section partly addresses *RQ5*. For the app adversary, the FE and BM models outperform the EG and HJ models. For BM, 14 out of 20 and for FE, 17 out of 20 app models provides  $\geq 95\%$  accuracy. Conversely, only 5 out of 20 app models provide  $\geq 90\%$  accuracy for EG. This is intuitive since BM and FE cover more activities than EG. HJ shows the lowest accuracy among the four sensor groups: 9 among 20 app models provide 70–90% accuracy. Both app and device models for EG and HJ require longer sub-session times (see *RQ2* of Sections 5.1-5.4) than BM and FE.

**5.5.3. Important Sensors per App Group.** All sensors remain active during data collection, yet certain apps have higher activity in some sensors. Next, we investigate *RQ5*: which sensor groups are important for which app groups.

**Body Motion.** Most app groups require BM data, *e.g.*, social apps involve walking, waving, and grabbing objects by users. Most of the group models provide  $\geq 85\%$  accuracy for BM. However, BM is not important for Teleport. group since teleportation doesn't involve significant body movement, thus providing only 70 – 80% accuracy (see Table 2).

**Eye Gaze.** For EG, no app-specific activity is identified. However, we assume that some apps require more eye-object interactions *i.e.*, in shooting & archery and rhythm groups, users aim at an object to shoot/cut it; thus, their EG models provide higher identification accuracy (85 – 95%). Conversely, certain app groups require minimal eye-object interaction (*e.g.*, knuckle-walking, golfing); thus, their accuracy is relatively lower (70 – 80%).

**Hand Joints.** HJ models for certain app groups that require active hand movements/gestures (*e.g.*, archery, flight simulation, interactive navigation, and rhythm) provide higher accuracy (see Table 2), *e.g.*, for flight-simulation apps that require users to control an airplane's control stick using hands, the models provide 75 – 80% accuracy. Conversely, HJ models for teleportation apps that require minimal hand movements achieve only 35 – 45% accuracy.

**Facial Expression.** FE is important in most app groups as various arousal/valence states can trigger specific facial expression. Consequently, FE models achieve  $\geq 90\%$  accuracy across all app groups. However, please note that face tracking is optional and can be disabled by users.

**Key Takeaways.** Models perform better if adversaries consider the most important sensor groups w.r.t. the activity of the app group. FE performs the best across all sensor groups.

## 6. Related Work

**Privacy in VR.** Adams et al. studied the awareness of users and developers on data collection practices on VR devices [1]. Trimananda et al. [57] analyzed the network traffic generated by popular apps on Oculus VR, and reported that personal information (device and user identifiers, parameters for fingerprinting, and some VR sensory data) is collected, and often in ways that are inconsistent with the statements in their privacy policies [57]. Nair et al. developed an app with tasks designed to demonstrate that it is possible to harvest users' personal information and also infer attributes, such as physical characteristics, location, and languages [42].

The privacy of sensor data and APIs receives increasing attention. For example, Kaleido proposed a DP-based defense of the privacy of eye tracking data, with focus on user interests as captured by eye gaze heatmaps [29]. Judith et al. compared emotion recognition in people with Parkinson's disease and health controls using dynamic facial expression and eye tracking [3]. VREED introduced a multimodal dataset demonstrating advanced emotion recognition in VR through eye tracking and physiological signals [55].

**User Identification in VR.** Most closely related to this paper is a body of prior work that focuses on identifying users based on sensor data collected on VR devices [11], [31], [39], [40], [42], [43], [46], [56], [62]. Most prior work focused on identifying users using body motion sensor data within pre-defined tasks/custom apps. In [53], Stephenson et al. compared various authentication mechanisms for AR/VR devices, which include head/hand/eye biometrics. Tricomi et al. identified users in VR/AR based on body motion and eye movements [56]. Pfeuffer et al. focused on user identification in various controlled tasks (*i.e.*, pointing, grabbing, walking, typing), including a technique that correlated body and eye tracking [46]. Miller et al. used features that correlate headset and controllers for user identification [40]. Miller et al. used body motion data to uniquely identify users as they watch randomly selected videos on VR device [39]. Nair et al. [43] analyzed a large dataset (50K users) of one real-world app (the popular Beat Saber game [17]), provided by the BeatLeader scoreboard [47]. They used body motion and contextual features to perform user identification.

**Our Work in Perspective.** To the best of our knowledge, BEHAVR is the first to analyze user identification in VR comprehensively, *i.e.*, considering (1) all VR sensors available (including HJ and FE sensors, in addition to BM, EG); (2) data we collected from several real-world, unmodified apps (as opposed to a custom app with "adversarial" tasks specifically designed to elicit behavior that enables identification), and (3) considering identifiability within and across different apps. Our enabling factor is our novel use of the SteamVR setup with ALVR [2] that allows us to collect *all* sensor data on the device. We built upon the summarization of the VR sensor data stream, originally developed in [39] for body motion data and also used in [43], but we needed additional cleanup due to invalid blocks in our case.

## 7. Conclusion

**Summary.** We present BEHAVR, a framework for collecting and analyzing VR sensor data from four sensor groups. We applied it to Quest Pro, and conducted a user study where real users interacted with real-world VR apps. We build models that an adversary can use to identify a user within an app, across all apps on the device, or within a group of apps with similar activity. We show that these models perform well, and we compare and combine their performance across different sensor groups and apps. Furthermore, we investigate the minimum amount of time and top features for identification, and the importance of sensor groups depending on the activity of the apps or app groups.

**Future Directions.** First, we can increase the size of our user study, in terms of participants *and* apps, in order to assess identifiability in larger datasets. One direction is to combine the large scale (when publicly available) datasets, with the richness of in-person user studies, by validating one against the other. Second, while we have considered, so far, all data streams and features, an adversary might want to minimize its work by feature minimization, and leveraging

cross-spatial relationships. Third, a natural next step is to develop defense mechanisms guided by our observations. Finally, it is interesting to explore the implications of VR identifiability, beyond just VR, and into the real-world, e.g., when surveillance cameras can capture motion/eye/face data and match them towards users' profiles from VR.

## 8. Acknowledgements

We would like to thank Diana Romero, for her help with part of our VR app selection process. This work is supported by NSF award 1956393 and a gift from the Noyce Initiative, partially supported by NSF award CNS-2105084.

## References

- [1] Devon Adams, Alseny Bah, Catherine Barwulor, Nureli Musaby, Kadeem Pitkin, and Elissa M. Redmiles. Ethics Emerging: the Story of Privacy and Security Perceptions in Virtual Reality. In *SOUPS*, August 2018.
- [2] ALVR. ALVR - Air Light VR. <https://github.com/alvr-org/alvr>, 2023.
- [3] Judith Bek, Ellen Poliakoff, and Karen Lander. Measuring emotion recognition by people with parkinson's disease using eye-tracking with dynamic facial expressions. *Journal of Neuroscience Methods*, 331, 2019.
- [4] Tomislav Bezmalinovic. Meta Quest Store: 5 Things You (Probably) Didn't Know. <https://mixed-news.com/en/meta-quest-store-analysis/>, April 2023.
- [5] Ivan Blagojević. Virtual Reality Statistics. <https://99firms.com/blog/virtual-reality-statistics/>, April 2023.
- [6] Stéphane Bouchard and G Labonté-Chartrand. *Emotions and the emotional valence afforded by the virtual environment*. IntechOpen, 2011.
- [7] Fadi Boutros, Naser Damer, Kiran Raja, Raghavendra Ramachandra, Florian Kirchbuchner, and Arjan Kuijper. Iris and periocular biometrics for head mounted displays: Segmentation, recognition, and synthetic data generation. *Image and Vision Computing*, 104:104007, 2020.
- [8] Corinna Cortes and Vladimir Vapnik. Support-vector networks. *Machine learning*, 20(3):273–297, 1995.
- [9] Martin Degeling, Christine Utz, Christopher Lentzsch, Henry Hosseini, Florian Schaub, and Thorsten Holz. We value your privacy... now take some cookies: Measuring the gdpr's impact on web privacy. In *NDSS*, 2019.
- [10] Thomas G. Dietterich. Ensemble methods in machine learning. In Josef Kittler and Fabio Roli, editors, *Multiple Classifier Systems, First International Workshop, MCS 2000, Cagliari, Italy, June 21-23, 2000, Proceedings*, volume 1857 of *Lecture Notes in Computer Science*, pages 1–15. Springer, 2000.
- [11] Yuming Du, Robin Kips, Albert Pumarola, Sebastian Starke, Ali Thabet, and Artsiom Sanakoyeu. Avatars grow legs: Generating smooth human motion from sparse tracking inputs with diffusion model. *arXiv preprint arXiv:2304.08577*, 2023.
- [12] Paul Ekman and Wallace V. Friesen. *Facial Action Coding System: Manual*. 1978.
- [13] William Enck, Peter Gilbert, Byung-Gon Chun, Landon P. Cox, Jaeyeon Jung, Patrick McDaniel, and Anmol N. Sheth. TaintDroid: An Information-Flow Tracking System for Realtime Privacy Monitoring on Smartphones. In *OSDI*, Oct 2010.
- [14] European Union (EU). Regulation (EU) 2016/679 of the European Parliament and of the Council of 27 April 2016 on the Protection of Natural Persons with Regard to the Processing of Personal Data and on the Free Movement of Such Data (General Data Protection Regulation). <https://eur-lex.europa.eu/legal-content/EN/TXT/PDF/?uri=CELEX:32016R0679>, 2018.
- [15] Bryn Farnsworth. Facial Action Coding System (FACS) – A Visual Guidebook. <https://imotions.com/blog/learning/research-fundamentals/facial-action-coding-system/>, October 2022.
- [16] Jerome H Friedman. Greedy function approximation: a gradient boosting machine. *Annals of statistics*, pages 1189–1232, 2001.
- [17] Beat Games. Beat Saber. <https://www.beatsaber.com/>, 2023.
- [18] Gonzalo Munilla Garrido, Vivek Nair, and Dawn Song. Sok: Data privacy in virtual reality. *arXiv preprint arXiv:2301.05940*, 2023.
- [19] US Federal Government. § 46.111 Criteria for IRB approval of research (eCFR). <https://www.ecfr.gov/current/title-45/subtitle-A/subchapter-A/part-46/subpart-A/section-46.111>, April 2023.
- [20] The Khronos OpenXR Working Group. The OpenXR Specification. <https://registry.khronos.org/OpenXR/specs/1.0/html/xrspec.html>, April 2023.
- [21] The Khronos OpenXR Working Group. The OpenXR Specification: § 12.28. XR\_EXT\_eye\_gaze\_interaction. [https://registry.khronos.org/OpenXR/specs/1.0/html/xrspec.html#XR\\_EXT\\_eye\\_gaze\\_interaction](https://registry.khronos.org/OpenXR/specs/1.0/html/xrspec.html#XR_EXT_eye_gaze_interaction), April 2023.
- [22] The Khronos OpenXR Working Group. The OpenXR Specification: § 12.30. XR\_EXT\_hand\_tracking. [https://registry.khronos.org/OpenXR/specs/1.0/html/xrspec.html#XR\\_EXT\\_hand\\_tracking](https://registry.khronos.org/OpenXR/specs/1.0/html/xrspec.html#XR_EXT_hand_tracking), April 2023.
- [23] The Khronos OpenXR Working Group. The OpenXR Specification: § 12.31.6. Conventions of hand joints. <https://registry.khronos.org/OpenXR/specs/1.0/html/xrspec.html#convention-of-hand-joints>, April 2023.
- [24] The Khronos OpenXR Working Group. The OpenXR Specification: § 12.53.7. Conventions of blend shapes. [https://registry.khronos.org/OpenXR/specs/1.0/html/xrspec.html#\\_conventions\\_of\\_blend\\_shapes](https://registry.khronos.org/OpenXR/specs/1.0/html/xrspec.html#_conventions_of_blend_shapes), April 2023.
- [25] The Khronos OpenXR Working Group. The OpenXR Specification: § 2.16. Coordinate System. <https://registry.khronos.org/OpenXR/specs/1.0/html/xrspec.html#coordinate-system>, April 2023.
- [26] Sepp Hochreiter and Jürgen Schmidhuber. Long short-term memory. *Neural computation*, 9(8):1735–1780, 1997.
- [27] Meta Inc. Supplemental Meta Platforms Technologies Privacy Policy. <https://www.meta.com/legal/privacy-policy/>, May 2023.
- [28] Peter Kuppens, Francis Tuerlinckx, James A Russell, and Lisa Feldman Barrett. The relation between valence and arousal in subjective experience. *Psychological bulletin*, 139(4):917, 2013.
- [29] Jingjie Li, Amrita Roy Chowdhury, Kassem Fawaz, and Younhyun Kim. Kaleido: Real-time privacy control for eye-tracking systems. In Michael Bailey and Rachel Greenstadt, editors, *30th USENIX Security Symposium, USENIX Security 2021, August 11-13, 2021*, pages 1793–1810. USENIX Association, 2021.
- [30] Andy Liaw and Matthew Wiener. Classification and regression by randomforest. *R News*, 2(3):18–22, 2002.
- [31] Jonathan Liebers, Mark Abdelaziz, Lukas Mecke, Alia Saad, Jonas Auda, Uwe Gruenefeld, Florian Alt, and Stefan Schneegass. Understanding User Identification in Virtual Reality through Behavioral Biometrics and the Effect of Body Normalization. In *Proceedings of the 2021 CHI Conference on Human Factors in Computing Systems*, pages 1–11, 2021.
- [32] Gilles Louppe. *Understanding Random Forests: From Theory to Practice*. PhD thesis, University of Liège, Belgium, 2014.
- [33] Meta. Bring your teams together in Meta Horizon Workrooms. [https://www.meta.com/work/workrooms/?utm\\_source=www.usenix.org&utm\\_medium=oculusredirect](https://www.meta.com/work/workrooms/?utm_source=www.usenix.org&utm_medium=oculusredirect), 2023.

- [34] Meta. Eye tracking on Meta Quest Pro. <https://www.meta.com/help/quest/articles/getting-started/getting-started-with-quest-pro/eye-tracking/>, 2023.
- [35] Meta. Getting started with Hand Tracking on Meta Quest headsets. <https://www.meta.com/help/quest/articles/headsets-and-accessories/controllers-and-hand-tracking/hand-tracking-quest-2/>, 2023.
- [36] Meta. Our story: enter the future of learning. <https://about.meta.com/immersive-learning/our-story/>, 2023.
- [37] Meta. This is Meta Quest Pro. <https://www.meta.com/quest/quest-pro/tech-specs/>, 2023.
- [38] Meta. Use Natural Facial Expressions on Meta Quest Pro. <https://www.meta.com/help/quest/articles/getting-started/getting-started-with-quest-pro/facial-expressions/>, 2023.
- [39] Mark Roman Miller, Fernanda Herrera, Hanseul Jun, James A Landay, and Jeremy N Bailenson. Personal Identifiability of User Tracking Data During Observation of 360-degree VR Video. *Scientific Reports*, 10(1):1–10, 2020.
- [40] Robert Miller, Natasha Kholgade Banerjee, and Sean Banerjee. Combining Real-world Constraints on User Behavior with Deep Neural Networks for Virtual Reality (VR) Biometrics. In *2022 IEEE Conference on Virtual Reality and 3D User Interfaces (VR)*, pages 409–418. IEEE, 2022.
- [41] Hooman Mohajeri Moghaddam, Gunes Acar, Ben Burgess, Arunesh Mathur, Danny Yuxing Huang, Nick Feamster, Edward W Felten, Prateek Mittal, and Arvind Narayanan. Watching You Watch: The Tracking Ecosystem of Over-the-Top TV Streaming Devices. In *ACM CCS*, 2019.
- [42] Vivek Nair, Gonzalo Munilla Garrido, Dawn Song, and James F. O’Brien. Exploring the Privacy Risks of Adversarial VR Game Design. In *Proceedings on Privacy Enhancing Technologies (PoPETs)*, 2023.
- [43] Vivek Nair, Wenbo Guo, Justus Mattern, Rui Wang, James F O’Brien, Louis Rosenberg, and Dawn Song. Unique Identification of 50,000+ Virtual Reality Users from Head & Hand Motion Data. *arXiv preprint arXiv:2302.08927*, 2023.
- [44] PR Newswire. Virtual Reality (VR) In Healthcare Global Market Report 2023: Virtual Reality Gains Acceptance in Remote Home Assessments. <https://finance.yahoo.com/news/virtual-reality-vr-healthcare-global-030000025.html>, 2023.
- [45] Andrew Paverd, Andrew Martin, and Ian Brown. Modelling and automatically analysing privacy properties for honest-but-curious adversaries. *Tech. Rep.*, 2014.
- [46] Ken Pfeuffer, Matthias J Geiger, Sarah Prange, Lukas Mecke, Daniel Buschek, and Florian Alt. Behavioural Biometrics in VR: Identifying People from Body Motion and Relations in Virtual Reality. In *Proceedings of the 2019 CHI Conference on Human Factors in Computing Systems*, pages 1–12, 2019.
- [47] Viktor Radulov. BeatLeader. <https://www.beatleader.xyz/>, July 2023.
- [48] Anastasia Shuba, Athina Markopoulou, and Zubair Shafiq. NoMoAds: Effective and Efficient Cross-App Mobile Ad-Blocking. In *PETS*, 2018.
- [49] State of California Department of Justice - Office of the Attorney General. California consumer privacy act (ccpa). [https://leginfo.ca.gov/faces/codes\\_displayText.xhtml?lawCode=CIV&division=3.&title=1.81.5.&part=4](https://leginfo.ca.gov/faces/codes_displayText.xhtml?lawCode=CIV&division=3.&title=1.81.5.&part=4), 2018.
- [50] Steam. CHARTS OVERVIEW. <https://store.steampowered.com/charts/>, April 2023.
- [51] Steam. Virtual Reality Titles. <https://store.steampowered.com/vr/>, July 2023.
- [52] SteamDB. Most played VR games. <https://steamdb.info/charts/?tagid=21978>, February 2023.
- [53] Sophie Stephenson, Bijeeta Pal, Stephen Fan, Earlence Fernandes, Yuhang Zhao, and Rahul Chatterjee. Sok: Authentication in augmented and virtual reality. In *2022 IEEE Symposium on Security and Privacy (SP)*, pages 267–284. IEEE, 2022.
- [54] Nazmi Sofian Suhaimi, Chrystalle Tan Bih Yuan, Jason Teo, and James Mountstephens. Modeling the affective space of 360 virtual reality videos based on arousal and valence for wearable eeg-based vr emotion classification. In *2018 IEEE 14th International Colloquium on Signal Processing & Its Applications (CSPA)*, pages 167–172. IEEE, 2018.
- [55] Luma Tabbaa, Ryan Searle, Saber Mirzaee Bafti, Md. Moinul Hosain, Jitrapol Intarasirisawat, Maxine Glancy, and Chee Siang Ang. VREED: virtual reality emotion recognition dataset using eye tracking & physiological measures. *Proc. ACM Interact. Mob. Wearable Ubiquitous Technol.*, 5(4):178:1–178:20, 2021.
- [56] Pier Paolo Tricomi, Federica Nenna, Luca Pajola, Mauro Conti, and Luciano Gamberini. You Can’t Hide Behind Your Headset: User Profiling in Augmented and Virtual Reality. *arXiv preprint arXiv:2209.10849*, 2022.
- [57] Rahmadi Trimananda, Hieu Le, Hao Cui, Janice Tran Ho, Anastasia Shuba, and Athina Markopoulou. {OVRseen}: Auditing network traffic and privacy policies in oculus {VR}. In *31st USENIX security symposium (USENIX security 22)*, pages 3789–3806, 2022.
- [58] Unity. Eye Gaze Interaction. <https://docs.unity3d.com/Packages/com.unity.xr.openxr@1.0/manual/features/eyegazeinteraction.html>, April 2023.
- [59] Valve. Steam Store. <https://store.steampowered.com/>, 2023.
- [60] Valve. SteamVR. <https://store.steampowered.com/app/250820/SteamVR/>, 2023.
- [61] Janus Varmarken, Hieu Le, Anastasia Shuba, Athina Markopoulou, and Zubair Shafiq. The TV is Smart and Full of Trackers: Measuring Smart TV Advertising and Tracking. In *PETS*, 2020.
- [62] Alexander Winkler, Jungdam Won, and Yuting Ye. QuestSim: Human Motion Tracking from Sparse Sensors with Simulated Avatars. In *SIGGRAPH Asia 2022 Conference Papers*, pages 1–8, 2022.
- [63] Yash and Jibin. Apple Vision Pro features, specs, price, and release date. <https://www.igeeksblog.com/apple-vision-pro-features/>, June 2023.

## Appendix A. List of SteamVR Apps

In Section 3, we discuss our experimental setup that includes how we choose 20 SteamVR apps from the list of top 100 SteamVR apps. In this appendix, Table 4 lists the 20 SteamVR apps and the description of app-specific activity that users perform during data collection.

## Appendix B. Data Summarization & Model Training

In Section 4.2, we discuss how we build BEHAVR models. In this appendix, we provide insights into optimizing FBA and selecting RF and XGB as ML algorithms for user identification in BEHAVR.

### B.1. FBA Evaluation and Optimization

First we shows the comparative analysis between FBL and FBA in Figures 6a, 6b, 6c and 6d. We can observe

TABLE 4: List of 20 VR apps in the BEHAVR app corpus.

App No.	App Title	Tasks
$a_1$	Beat Saber	Play the tutorial; in the middle, the user is prompted to play the tutorial again with bare hands.
$a_2$	BONEWORKS	Explore the welcome scene; in front of a shelf, the user is prompted to grab dumbbells with bare hands, and perform bicep curls.
$a_3$	DCS World Steam Edition	Fly a military aircraft; in the middle, the user is prompted to control the aircraft with bare hands.
$a_4$	Deraill Valley	Explore the welcome scene in a train station; in front of a table, the user is prompted to move a book and a walkie-talkie using bare hands.
$a_5$	Elven Assassin	Shoot arrows in three scenes: twice with the controllers and once with bare hands.
$a_6$	Golf It!	Putt a golf ball with the controllers; once it gets really close to the hole, the user is prompted to continue with bare hands.
$a_7$	Gorilla Tag	Perform gorilla movement with the controllers; in the middle, the user needs to perform the same movement with bare hands.
$a_8$	Hot Dogs, Horseshoes & Hand Grenades	Explore one scene of a park; in front of a vending machine, the user is prompted to interact with it with bare hands.
$a_9$	Job Simulator	Explore one scene of an office-worker simulation; in the middle, the user is prompted to interact with a desktop PC with bare hands.
$a_{10}$	Keep Talking and Nobody Explodes	Explore one scene of a bomb defuse with controllers; in the middle, the user is prompted to defuse the bomb with bare hands.
$a_{11}$	McOsu	Explore the welcome scene; in the middle, the user is asked to interact with the virtual objects with bare hands.
$a_{12}$	Neos VR	Explore a scene in a futuristic building; in the middle, the user is prompted to interact with books in a bookshelf with bare hands.
$a_{13}$	No Man’s Sky	Explore an unknown planet by teleporting and interacting with a laser gun; in the middle, the user is prompted to interact with the gun with bare hands.
$a_{14}$	Pavlov VR	Play the basic and shooting tutorials; for hand motion, the user is prompted to interact with a panel with bare hands.
$a_{15}$	Rec Room	Explore the welcome scene in a school by going around the building; in the middle, the user is prompted to wave their hands at an avatar with bare hands.
$a_{16}$	Space Engine	Explore a virtual planetarium by teleporting to five space objects ( <i>e.g.</i> , planets, stars, etc.); in the middle, the user is asked to interact with the planetarium with bare hands.
$a_{17}$	Tabletop Simulator	Move chess pieces with the controllers; in the middle, the user is prompted to move chess pieces back with bare hands.
$a_{18}$	VRChat	Explore the welcome scene by walking around; in the middle, the user is prompted to wave at themselves in front of a mirror.
$a_{19}$	VTOL VR	Play the basic tutorial for flying a helicopter; in the middle, the user is prompted to interact with the control stick with bare hands.
$a_{20}$	X-Plane 11	Fly a civilian aircraft and interact with the virtual objects with controllers and with bare hands.

TABLE 5: Feature dimensions for summarized sensor data (in tabular format) using the FBA method. For each sensor group and value of  $r$  we report the (number of blocks, number of features)

Sensor Group	$r = 2$	$r = 1$	$r = 0.5$	$r = 0.2$	$r = 0.1$
Body Motion	(150658, 165)	(75342, 165)	(37834, 165)	(15133, 165)	(7468, 165)
Eye Gaze	(168400, 46)	(84200, 46)	(41920, 46)	(16520, 46)	(8080, 46)
Hand Joints	(58480, 500)	(29240, 500)	(14360, 500)	(5480, 500)	(2520, 500)
Facial Expression	(168400, 320)	(84200, 320)	(41920, 320)	(16520, 320)	(8080, 320)

TABLE 6: Performance analysis for algorithm selection (BM = body motion, EG = eye gaze, HJ = hand joints, FE = facial expression).

Alg.	App No.	Accuracy (%)			
		BM	EG	HJ	FE
RF	$a_1$	100	100	100	100
RF	$a_{15}$	100	100	100	100
XGB	$a_1$	100	100	100	100
XGB	$a_{15}$	85.71	85.71	71.42	100
SVM	$a_1$	57.14	57.14	85.71	100
SVM	$a_{15}$	38.23	38.23	71.42	38.23

that FBA gives improves app model identification accuracy (5–15% for body motion, 5–25% for eye gaze, and 5–10% for hand joints) for most apps compared to FBL.

**Choosing Optimal Ratio  $r$ .** The main challenge when using FBA is finding the optimal FBA block division ratio  $r$ . If  $r$  is too high, summarized data become noisy. On the contrary, if  $r$  is too low, important information would be missing from the summary. Finding the right balance is crucial to preserve relevant information. We perform a preliminary experiment based on 7 participants to find the optimal value of  $r$ . For body motion and eye gaze, the results suggest  $r = 1$ . For hand joints, the results suggests  $r = 0.5$ ; this is intuitive as a meaningful hand gesture can be captured in a longer

block length. For facial expression, the results suggest that any  $r$  values will be optimal. Thus, to align  $r$  values across all sensor groups, we choose  $r = 1$ .

**Data Summarization Output.** Table 5 presents the dimensions of the output of data summarization using FBA.

## B.2. Algorithm Selection

We initially explore various ML models such as Random Forest (RF) [30], Gradient Boosting (XGB) [16], Support Vector Machine (SVM) [8], and Long Short-Term Memory Networks(LSTM) [26] across two apps : consist of one social app, namely Rec Room ( $a_{15}$ ), and rhythm app, namely Beat Saber ( $a_1$ ). We analyze the two apps (out of 20), which are among the most popular VR apps, as they contain common activities (*e.g.*, walking, waving, grabbing, etc.). Table 6 shows that RF achieves the highest identification accuracy; We argue that LSTM is intended to perform sequence prediction, whereas BEHAVR focuses on identification (*i.e.*, a classification task); LSTM performs poorly (~81% accuracy for body motion in app  $a_1$ ), thus, we do not consider LSTM further in our evaluation.



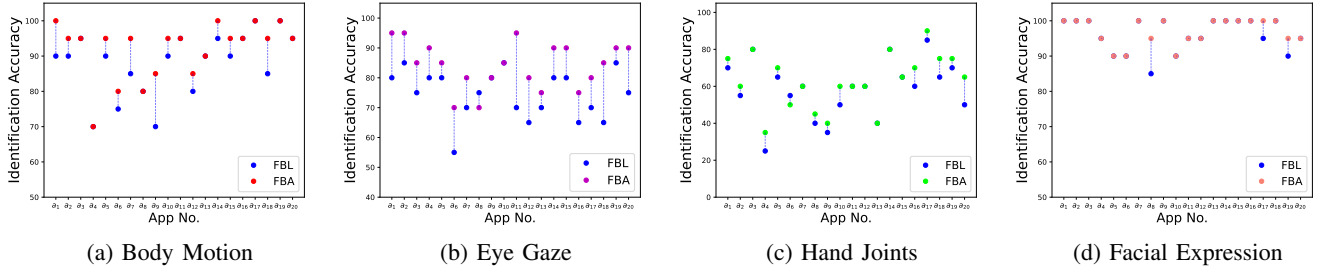


Figure 6: Identification accuracy comparison between FBA and FBL methods for the four sensor groups.

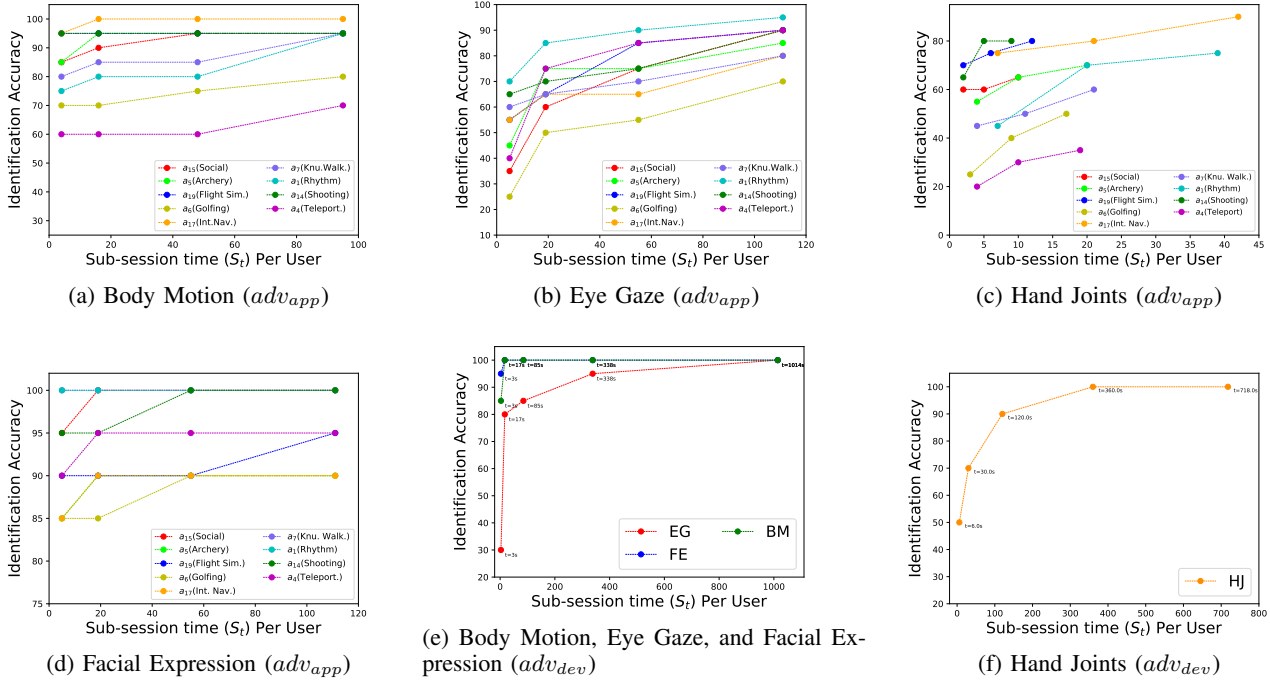


Figure 7: User identification accuracy for app models and device adversary w.r.t. average sub-session time ( $S_t$  in second) per user.

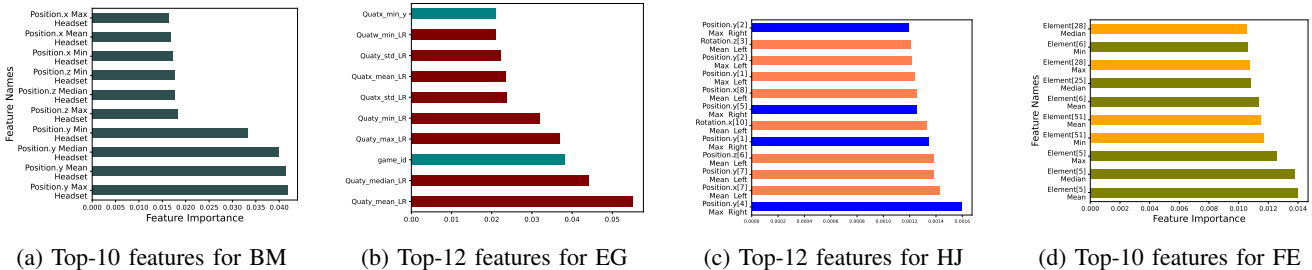
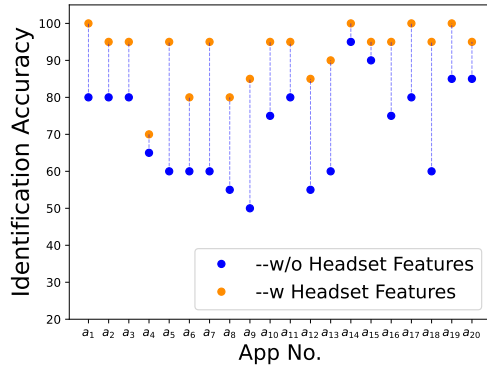


Figure 8: Top features for user identification for device adversary w.r.t. each of the four sensor groups (BM = body motion, EG = eye gaze, HJ = hand joints, FE = facial expression).

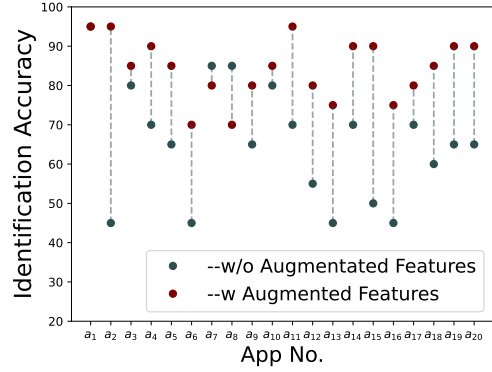
## Appendix C. More Evaluation Results

In Section 5, we discuss the evaluation results of BEHAVR’s app and device models for user identification. In

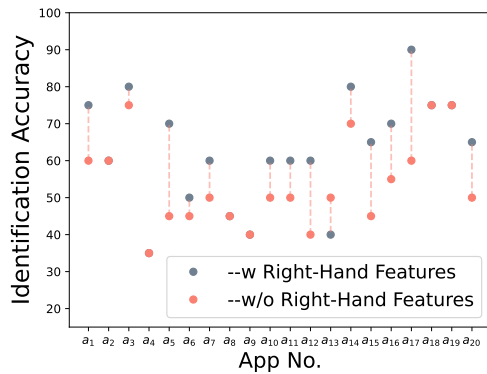
this appendix, we present tables and figures that give more details on the evaluation.



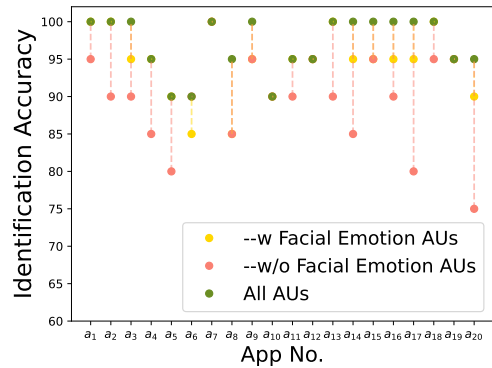
(a) Headset features of BM



(b) Augmented features of EG



(c) Right-hand features of HJ



(d) Emotion AUs of FE

Figure 9: Visualization of identification accuracy improvement for various sensor groups w.r.t. top-features.

### C.1. Sub-session Time Characterization

Figures 7a, 7b, 7c, and 7d (for app adversary); and Figures 7e and 7f (for device adversary) show identification accuracy w.r.t. sub-session time.

### C.2. Top Features

We list the top features for user identification using app models trained with data from the four sensor groups in Tables 7. Further, Figures 8a, 8b, 8c, and 8d show the top features for user identification for device adversary.

#### Identification Accuracy Improvement by Top Features.

In Figure 9a, 9b, 9c and 9d shows importance of headset features for BM, augmented features for EG, right-hand features of HJ and Finally, AUs/elements of emotion for FE respectively.

TABLE 7: Top-3 features in user identification for app models for each of the four sensor groups.

App No.	Body Motion	Eye Gaze	Hand Joints	Facial Expression
$a_1$	Position.z Mean Left Controller, Position.z Min Headset', Position.y Median Right Controller	Quat.y Mean Left Right, Quat.y Median Left Right, Quat.y Max Left Right	Position.z[3] Max Right, Rotation.z[24] Mean Left, Position.z[1] Max Right	Element[23] Min, Element[5] Median, Element[6] Mean
$a_2$	Position.x Max Headset, Position.y Max Headset, Position.x Mean Headset	Quat.y Mean Left Right, Quat.y Median Left Right, Quat.x Mean Right	Position.z[26] Med Left, Rotation.z[2] Med Right, Rotation.z[18] Min Left	Element[5] Min, Element[57] Median, Element[5] Median
$a_3$	Position.x Mean Headset, Position.z Max Headset, Quat.y Median Headset	Quat.y Mean Left Right, Quat.y Mean Left, Quat.x Max Right	Quat.y Mean Left Right, Quat.y Max Left Right	Element[28] Min, Element[51] Min, Element[51] Median
$a_4$	Position.z Min Headset, Position.y Max Headset, Position.z Max Headset	Quat.y Max Left Right, Quat.y Mean Left Right, Rotation.w Med Left	Position.y Mean Right, Rotation.z[25] Max Right, Position.x[26] Mean Right	Element[30] Min, Element[29] Mean, Element[29] Min
$a_5$	Position.y Min Left Controller, Lin.0 Std Right Controller, Quat.z Mean Right Controller	Quat.y Min Left Right, Quat.y Mean Left Right, Quat.y Max Left Right	Position.x Mean Right, Rotation.z[3] Max Left, Rotation.z[11] Med Left	Element[6] Min, Element[57] Mean, Element[5] Mean
$a_6$	Position.x Min Headset, Position.x Max Headset, Quatw Max Headset	Quat.y Mean Left Right, Quat.y Median Left Right, Quatw Mean Left	Rotation.z Min Left, Rotation.x Max Left, Position.y Max Right	Element[26] Min, Element[57] Mean, Element[5] Mean
$a_7$	Quat.w Mean Headset, Position.x Mean Headset, Quat.x Min Right Controller	Quat.y Mean Left Right, Quat.y Median Left Right, Quat.y Max Left Right	Position.x Mean Left, Position.z Max Left, Rotation.y Min Left	Element[5] Median, Element[2] Min, Element[6] Median
$a_8$	Position.y Max Headset, Position.y Mean Headset, Position.y Median Headset	Quat.y Mean Left Right, Quat.y Median Left Right, Quat.y Max Left Right	Rotation.z Max Right, Rotation.x Mean Right, Position.x Min Right	Element[30] Min, Element[29] Min, Element[6] Median
$a_9$	Quat.y Min Right Controller, Position.x Mean Right Controller, Quat.x Max Right Controller	Quat.y Mean Left Right, Quat.y Median Left Right, Quat.y Max Left Right	Position.z Max Left, Position.y Mean Right, Position.z[2] Max Left	Element[30] Min, Element[6] Mean, Element[27] Max
$a_{10}$	Position.x Median Headset, Position.x Max Headset, Position.x Mean Headset	Quat.y Mean Left Right, Quat.y Median Left Right, Quatw Mean Left	Position.y Mean Right, Rotation.y[12] Min Left, Rotation.z[6] Max Left	Element[29] Min, Element[25] Min, Element[2] Min
$a_{11}$	Position.y Max Headset, Position.y Mean Headset, Position.x Min Headset	Quat.y Mean Left Right, Quat.y Median Left Right, Quat.y Max Left Right	Position.z Min Left, Position.x[11] Max Right, Position.x Mean Left	Element[51] Min, Element[51] Median, Position.x Mean Left
$a_{12}$	Position.y Max Headset, Position.y Mean Headset, Position.y Min Headset	Quat.y Mean Left Right, Quat.y Median Left Right, Quat.y Max Left Right	Position.x Min Right, Position.x[24] Mean Right, Position.x[17] Min Right	Element[51] Median, Element[51] Min, Element[51] Mean
$a_{13}$	Position.y Max Headset, Position.x Mean Headset, Position.y Mean Headset	Quat.y Mean Left Right, Quat.y Median Left Right, Quat.y Min Left Right	Position.x Mean Right, Position.z[15] Min Right, Position.x[5] Mean Right	Element[51] Min, Element[6] Min, Element[25] Max
$a_{14}$	Quat.x Mean Right Controller, Position.z Min Left Controller, Quat.w Mean Left Controller	Quat.y Mean Left Right, Quat.x Max Left, Quatw Max Right	Position.x Mean Left, Position.y[24] Mean Left, Position.x[7] Med Right	Element[51] Median, Element[25] Median, Element[51] Min
$a_{15}$	Position.y Max Headset, Position.x Max Headset, Position.x Mean Headset	Quat.y Mean Left Right, Quat.y Median Left Right, Quat.y Max Left Right	Position.x Mean Right, Position.x[14] Mean Right, Position.x[6] Med Left	Element[51] Min, Element[23] Min, Element[25] Median
$a_{16}$	Position.y Max Headset, Position.x Min Headset, Position.x Mean Headset	Quat.y Mean Left Right, Quat.y Median Left Right, Quat.y Min Left Right	Position.z Min Left, Rotation.z[3] Med Left, Position.x[12] Mean Right	Element[25] Min, Element[5] Mean, Rotation.z[3] Med Left
$a_{17}$	Position.x Min Headset, Position.x Mean Headset, Position.y Max Headset	Quat.y Mean Left Right, Quat.y Median Left Right, Quat.y Max Left Right	Position.y Med Left, Rotation.z[22] Min Right, Rotation.x[25] Mean Right	Element[50] Min, Element[41] Mean, Element[54] Mean
$a_{18}$	Position.y Max Headset, Position.z Mean Headset, Position.y Median Headset	Quat.y Mean Left Right, Quat.y Median Left Right, Quat.x Mean Right	Position.z[13] Mean Right, Position.z[8] Max Left, Position.y[18] Med Left	Element[25] Median, Element[2] Min, Position.z[8] Max Left
$a_{19}$	Quat.x Min Right Controller, Quatw Max Left, Position.y Median Right Controller	Quat.y Mean Left Right, Quat.x Min Right, Quatw Max Left	Position.z Max Left, Position.z[18] Med Left, Position.y[1] Med Left	Element[51] Min, Element[51] Mean, Element[25] Median
$a_{20}$	Position.x Min Headset, Position.x Median Headset, Position.x Mean Headset	Quat.y Mean Left Right, Quat.y Median Left Right, Quat.y Max Left Right	position.x[11] Max Left, Position.x[12] Med Left, Position.x[4] Max Left	Element[30] Min, Element[30] Mean, Element[5] Mean